Schizophrenia Bulletin Open
https://doi.org/10.1093/schizbullopen/sgad019

Gene Expressions Preferentially Influence Cortical Thickness of Human Connectome Project Atlas Parcellated Regions in First-Episode Antipsychotic-Naïve Psychoses

Bridget N. McGuigan[1,#], Tales Santini[2,#], Matcheri S. Keshavan[3], and Konasale M. Prasad[*,1,2,4]

[1]University of Pittsburgh School of Medicine, University of Pittsburgh, Pittsburgh, PA, USA; [2]University of Pittsburgh Swanson School of Engineering, University of Pittsburgh, Pittsburgh, PA, USA; [3]Beth Israel Deaconess Medical Center, Harvard Medical School, Boston, MA, USA; [4]Department of Psychiatry, Veterans Affairs Pittsburgh Healthcare System, Pittsburgh, PA, USA

[*]To whom correspondence should be addressed; 3811 O'Hara St, Pittsburgh, PA 15213, USA; tel: +1 412-586-5014; e-mail: KMP8@Pitt.edu

[#]Contributed equally.

Altered gene expressions may mechanistically link genetic factors with brain morphometric alterations. Existing gene expression studies have examined selected morphometric features using low-resolution atlases in medicated schizophrenia. We examined the relationship of gene expression with cortical thickness (CT), surface area (SA), and gray matter volume (GMV) of first-episode antipsychotic-naïve psychosis patients (FEAP = 85) and 81 controls, hypothesizing that gene expressions often associated with psychosis will differentially associate with different morphometric features. We explored such associations among schizophrenia and non-schizophrenia subgroups within FEAP group compared to controls. We mapped 360 Human Connectome Project atlas-based parcellations on brain MRI on to the publicly available brain gene expression data from the Allen Brain Institute collection. Significantly correlated genes were investigated using ingenuity pathway analysis to elucidate molecular pathways. CT but not SA or GMV correlated with expression of 1137 out of 15 633 genes examined controlling for age, sex, and average CT. Among these ≈19%, ≈39%, and 8% of genes were unique to FEAP, schizophrenia, and non-schizophrenia, respectively. Variants of 10 among these 1137 correlated genes previously showed genome-wide-association with schizophrenia. Molecular pathways associated with CT were axonal guidance and sphingosine pathways (common to FEAP and controls), selected inflammation pathways (unique to FEAP), synaptic modulation (unique to schizophrenia), and telomere extension (common to NSZ and healthy controls). We demonstrate that different sets of genes and molecular pathways may preferentially influence CT in different diagnostic groups. Genes with altered expressions correlating with CT and associated pathways may be targets for pathophysiological investigations and novel treatment designs.

Key words: Gene expression/schizophrenia/cortical thickness/surface area/gray matter volume/neuroimaging

Introduction

Despite high heritability of schizophrenia (SZ)[1,2] and replicated genome-wide association of many gene variants,[3] pathophysiological mechanisms associated with genetic factors are unclear. Heritability of regional morphometry,[4] white matter diffusivity,[5] and functional activation[6] have been reported. Many studies have associated genetic variants with alterations in morphometry of specific regions,[7–11] functional brain variations,[12] widespread functional connectivity,[13] and also, with treatment outcomes.[14–16] Recent findings associate variants of genome-wide significance, e.g. variants on the *Zinc Finger Protein 804A* (*ZNF804A*)[17] and on *Calcium voltage-gated channel subunit alpha1 C* (*CACNA1C*) with decreased total and frontal white matter volume.[18,19] Recent studies have reported convergence of schizophrenia risk genes on limbic and ventral networks[20] and on certain brain regions associated with pathophysiology of schizophrenia but not in tissues of less relevance to SZ.[21] A genetically patterned consolidation of anatomical network hubs may underlie normative brain maturation, and many genes loading into these components were overrepresented in risk genes for SZ.[22] For these reasons, examining the association of gene expressions with brain morphometry could enhance our understanding of the neurobiology of SZ.

Recent efforts in associating publicly available gene expression data to brain imaging measures show correlations between SZ risk gene expressions with white matter dysconnectivity.[23] Correlation of neuronal calcium signaling, which included *CACNA1C*,[23] and astrocyte-specific gene markers were associated with cortical thinning in SZ.[24] The roles of specific neuronal cell types on cortical thickness (CT) changes have been recently examined in SZ[25,26] and in gray matter volume (GMV) in drug-naive first-episode SZ.[27] Existing studies have used the Desikan–Killiany-Tourville Atlas that produces larger parcellations based on anatomical landmarks and have mainly examined medicated patients with longer duration of illness. Further, these studies have examined either CT or GMV.[23,24] Since CT and surface area (SA) may be differentially regulated during development,[28–30] and volume as a product of SA and CT may be affected by combined variations in CT and SA, examining GMV, CT, and surface (SA) individually may not provide comprehensive understanding of the relationship of altered gene expressions with cortical morphology.

To address these concerns, we examined a cohort of first-episode antipsychotic-naïve psychosis (FEAP) patients for all three morphometric features (CT, SA, and GMV) in relation to publicly available gene expression data from the Allen Human Brain Atlas (AHBA) repository to gain a comprehensive understanding of morphometric variations and minimize the confounds of medication effects on morphometry and longer duration of illness. Brain regions were parcellated into 360 anatomically and functionally connected regions[31] using the Human Connectome Project (HCP)-atlas providing more granular information on the association of brain regions with gene expressions. An additional rationale behind using the HCP atlas was to use the results of this manuscript to investigate structural and functional connectome related to the transcriptome changes in the future. To understand the contribution of gene expression differences to the morphometric features of brain regions showing significant case–control differences, we examined these regions first followed by all regions irrespective of whether they showed group differences or not. We predicted that the regions that show the main effect of disease on each of the morphometric features will show stronger correlation with schizophrenia risk genes compared to regions without the main effect. In order to enhance the reproducibility, we have used a standardized workflow and guidelines for "imaging transcriptomics."[32,33] Based on existing literature, we hypothesized that gene expressions regulating molecular pathways often associated with psychosis such as synaptic function and plasticity, ion channels, inflammation, glutamatergic neurotransmission, oxidative stress, and cerebral bioenergetic pathways will correlate with morphometric features.[23,24,34–36] Many of the genes regulating these biological processes have been associated with SZ.[22,37]

Methods

Clinical Data

We enrolled 92 young-adult FEAP patients and 81 healthy controls (HC) of both sexes, diagnosed per DSM-IV from the inpatient and outpatient facilities of the Western Psychiatric Institute and Clinic, Pittsburgh, PA, USA. Exclusion criteria were the presence of significant medical/neurological disorders, prior/current antipsychotic treatment, substance dependence within the past 6 months or abuse in the last month and mental retardation per DSM-IV. Senior clinicians provided the consensus diagnosis after reviewing medical records, the Structured Clinical Interview for DSM-IV (SCID-IV) data, and at least 6-month follow-up information. The University of Pittsburgh Institutional Review Board approved the study. All subjects gave informed consent after a complete description of the study.

MRI Methods

T1-weighted data were acquired using a 1.5T whole-body scanner using three-dimension spoiled gradient recalled (SPGR), steady-state pulse sequence (124 coronal slices, 1.5 mm thickness, acquisition matrix = 256 × 192). Details of acquisition are published.[38]

HCP-Atlas-Based Parcellations

The MRIs were processed using the Freesurfer package 7.1.0, and then the segmentations were mapped onto the HCP atlas using Freesurfer version of HCP-MMP 1.0 parcellation[39,40] in "*fsaverage*" space.[41] The parcellations from all subjects were visually inspected for white matter/gray matter/subcortical boundaries. Seven FEAP subjects were excluded from the study due to poor image quality (partial coverage = 5; truncated area = 1; skull captured as pial = 1).

The Allen Human Brain Atlas

Microarray expression data from 6 healthy donors (2 African American males aged 24 and 39 years, two Caucasian males aged 57 and 31 years, 48-year-old Caucasian female, and 49-year-old Hispanic female) were used in this study. Tissue samples were obtained from both hemispheres for 2 donors and from the left hemisphere for the rest. The total number of tissue samples obtained per donor varied from 363 to 948 per brain. Some regions were sampled more than once (e.g. right Fusiform Face Complex sampled 35 times) while others were sampled once (e.g. left Posterior Insula). Samples from subcortical regions, e.g. amygdala and substantia nigra were not included in the analysis, since there is no clear definition of CT for these regions. The AHBA used 58 692 probes to obtain gene expression levels for each brain sample, which corresponds to 15 633 unique genes (several genes had multiple probes).

Mapping AHBA Data to HCP Atlas

The AHBA used blockface images of histological tissue slabs to map the gene expression onto MRI within the Montreal Neurological Institute space. The gene expression data from the tissue sample coordinates were mapped onto the HCP atlas using the ABAGEN toolbox[33] resulting in 283 out of 360 HCP cortical regions with a corresponding tissue sample. The probes were selected using "differential stability," where, for each gene, the probe with the highest mean correlation among the donors was chosen for the analysis.[42] The gene expression data were then normalized to reduce within-donor variability and outliers using the scaled sigmoidal transformation method[43] and mapped onto the 283 cortical regions in the HCP atlas in Montreal Neurological Institute space. If multiple samples were mapped into one region, they were first averaged by donor and then averaged among all donors, giving the resultant gene expression value for that region (Fig 1). The methods we used for probe selection and data normalization have been shown to provide the most accurate gene expression dataset using the AHBA database.[32]

Data Analysis

Case–control differences for each morphometric feature was examined using MANCOVA including age and sex as covariates followed by Bonferroni-corrected between-subjects effects. Total GMV, total SA, and mean CT across all the included regions were additional covariates for the comparison of total GMV, SA, and CT, respectively.

Next, we examined the correlation of gene expression with morphometry of regions showing significant case–control differences, followed by examining correlation with all regions regardless of group differences. We constructed a 2D matrix for each morphometry (CT, SA, GMV). Rows of each matrix consisted of HCP regions (n = 283) while the columns consisted of subjects (85 FEAP and 81 controls; sample after quality check) and 15 633 genes (totaling 15 799 columns). Partial correlations were then applied for each of these matrices separately between 283 HCP regions and 15,633 gene expressions, controlling for age, sex, average CT, total SA, or total GMV depending on the morphometric feature examined. Thus, this resulted in a correlation matrix of 166 subjects × 15 633 genes for each morphometric measure. The observed power was 0.81 with a sample of 166 (85 FEAP and 81 HC) for 2-way significance at $P < .05$ assuming an r = 0.22 and three covariates (SPSS V 28.0.1.1). Multiple testing was corrected using the Benjamini-Hochberg approach of the false discovery rate.[44] We also examined the differences in the strength of correlation between the groups using z-transformed partial r for significant gene expression values common between patients and controls with each morphometric measure using MANOVA. The Bonferroni-corrected between-subjects effects are reported for each morphometric measure.

To understand the functional implication of correlated gene expressions, we examined the biological pathways with which these genes were associated using the QIAGEN ingenuity pathway analysis. The pathways for each dataset were utilized to find statistically significant canonical pathways, based on the P-value of overlap calculated by right-tailed Fisher's Exact Test.[45]

Next, we grouped the FEAP sample into SZ and non-schizophrenia (NSZ) subsamples to explore whether correlation of gene expressions is different in these diagnostic groups using the methods described above. SZ group included schizophrenia (n = 47) and schizoaffective disorder (n = 6). NSZ included delusional disorder (n = 2), unspecified psychotic disorder (n = 12), major depressive disorder (n = 14), and bipolar disorder (n = 4).

Results

Clinical and Demographic Data

The final dataset, after checking quality, consisted of 85 FEAP and 81 HC (see table 1 for DSM-IV diagnostic composition of the FEAP). Age, total GMV, mean CT, and total SA did not differ between the groups. There were significantly more males among patients compared to controls (P = .01).

Between-Group Morphometric Differences

The Bonferroni-corrected between-subjects effects of the MANCOVA model showed significant alterations in CT and SA of approximately 5% of regions each and GMV of 10% of regions between FEAP and control groups. The differences were of small effect sizes. Most of these regions showed reduction in CT, SA, or GMV in the FEAP group compared to controls. Of these regions, 7 showed significant differences in both SA and GMV while 7 others showed significant differences in CT and GMV (table 2). No region was significant in all 3 metrics. Many regions showing morphometric differences were located in the prefrontal (dorsolateral prefrontal, medial prefrontal, inferior frontal, anterior cingulate, and orbitofrontal cortex), temporal (lateral temporal and belt complexes), and parietal (inferior and superior parietal) areas. Overall MANCOVA models for each morphometric feature; however, were not significant (CT: Wilk's λ = 0.005, F = 1.24, P = .63; SA: Wilk's λ = 0.005, F = 1.18, P = .64; GMV: Wilk's $\lambda < 0.001$, F = 16.42, P = .20).

SZ showed a similar pattern of morphometric changes compared to controls. Among SZ patients, the right Area TE1 posterior (TE1p) in the lateral temporal cortex and left Area PGs in the inferior parietal cortex, showed significant differences in all 3 metrics (supplementary table 1). However, NSZ showed changes in CT and SA in about 2% of the regions and in GMV in about 3% of regions compared to

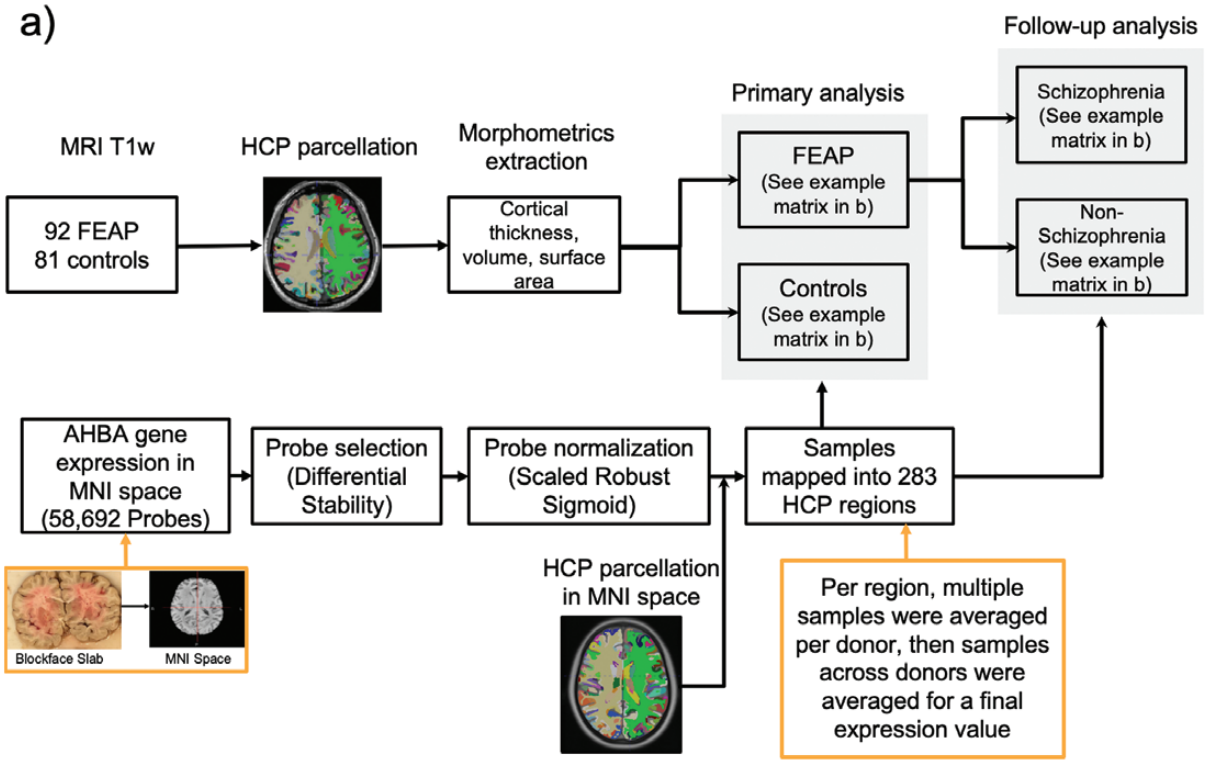

Fig 1. a) Schematic of the analysis pipeline. MRI data of FEAP and healthy controls (HC) subjects were processed for regional morphometrics after excluding those with artifacts. HCP-atlas was used to parcellate the regions. Gene probes were selected, normalized, and mapped onto the parcellated regions. Gene expressions from the probes were correlated with the morphometrics between FEAP and HC subjects first, then between SZ and NSZ second. Sample size of FEAP and HC represents total subjects before quality check of the MRI and HCP parcellations. b) Representative matrix for correlation of gene expressions with morphometry of ROI.

controls. No region was different in all 3 morphometrics among the NSZ group relative to controls (supplementary table 2). Among the regions that showed significant morphometric differences, CT of one region (left anterior 32 prime) and GMV of 5 regions (left superior frontal language area, left inferior 6–8 transitional area, left area PGs, right area TE1 posterior, right area TE2 posterior) were common between SZ and NSZ compared to controls.

Table 1. Clinical and Demographic Features

	FEAP (n = 85)	Healthy Controls (n=81)	t/χ2	p
Age(yr.), mean (SD)	24.08 (7.28)	24.7 (6.60)	0.57	.57
Sex, M/F	61/24	43/38	6.19	**.01***
Race, C/AA/H	58/21/1	61/16/1	2.66	.62
TBV, mean (SD) in cc	1192.77 (137.52)	1178.94 (105.82)	0.72	.47
Mean CT (SD) in mm	2.53 (0.10)	2.55 (0.08)	1.19	.24
Total SA (SD) in mm^2	176175.91 (18926.94)	173193.24 (14963.23)	1.12	.26
DSM-IV diagnoses	Schizophrenia 47 Schizoaffective disorder 6 Delusional disorder 2 Unspecified psychotic disorder 12 Major depressive disorder 14 Bipolar disorder 4			

Correlation of Regional Morphometry Showing Between-Group Differences With Gene Expression

None of the gene expressions showed false discovery rate-corrected correlations with CT, SA, or GMV of regions showing between-group differences in each metric and regions shown in table 2 and mentioned in the previous section.

Correlation of Gene Expressions With Morphometry of All Brain Regions Regardless of Group Differences

About 7% of the 15 633 genes showed false discovery rate-corrected correlations with CT, among which about 77% were common between the FEAP and HC. Proportionately more gene expressions (19.3%) were unique to FEAP while ≈3% were unique to HC (table 3; supplementary Table 3), and expression of significantly more genes was positively correlated among FEAP (61%) and HC (29%) ($\chi^2 = 4.43$, $P = .03$) (table 3; figure 2).

We observed a similar pattern when SZ was compared to HC, but comparatively more gene expressions (38.7%) were unique to SZ compared to HC (<1%) from 1,137 gene expressions significantly correlated with CT (supplementary table 4). In the NSZ-HC comparison, fewer total genes (n = 1006) correlated with CT with 89 (8.8%) gene expressions unique to NSZ while 143 (14.2%) were unique to HC (supplementary table 5).

Between SZ and NSZ, 1348 total gene expressions showed significant correlations of which 488 (36.2%) were unique to SZ and only 3 genes to NSZ, while the rest were common to both groups. (supplementary table 6).

Ten SZ risk genes reported in the recent GWAS study,[46] showed significant correlation of expression with CT. Expression of three genes, GRAM domain containing 1B (*GRAMDB1*), Hydroxypyruvate isomerase (*HYI*), and Mitogen-activated protein kinase 3 (*MAPK3*), correlated with CT in FEAP only. Expression of Ecto-NADPH Oxidase Disulfide-Thiol Exchanger 1 (*ENOX1*), Family with sequence similarity 216 members (*FAM216A*), KAT8 regulatory NSL complex subunit 1 (*KANSL1*), Kruppel-like factor 6, MLX Interacting protein (*MLXIP*), Phospholipase C Eta 2 (*PLCH2*), and Ribonuclease H2 Subunit C (*RNASEH2C*) correlated with CT in both FEAP and HC. Expression of none of these genes correlated with CT among controls.

In summary, expression of only a small proportion of genes significantly correlated with CT. SA and GMV did not significantly correlate with gene expressions. CT of FEAP subjects was associated with expression of relatively more genes compared to HC. A large majority of gene expression correlations were common to both groups. Among the gene expressions that were unique to each group in the subgroup analysis of SZ and NSZ compared to controls, a higher proportion of transcripts correlated with CT among SZ than among HC whereas CT of NSZ showed correlation with fewer genes than HC, or SZ. Only 10 of the significantly correlated genes were among those showing genome-wide association with schizophrenia in a recent study.[46]

Ingenuity Pathway Analysis Analysis

Pathways Unique to FEAP. A relatively higher number of pathways (n = 53) were identified for the 134 positively correlated gene expressions than for the 86 negatively correlated ones (n = 16). Some of the pathways of positively correlated gene expressions were inflammation (IL-17A signaling, JAK/STAT signaling, IGF-1 signaling [*JUN*, *MAPK3*], and complement system [*CQ1A, CQ1B*]), endocannabinoid pathway (*ADCY2, CNR1*) and synaptogenesis signaling pathway (*CDH2, SYT10*). Examples of pathways associated with negatively correlated gene expressions are inflammation (CXCR4 signaling [*RHOBTB2*], Chemokine signaling [*ROCK2*], IL-8 signaling, and VDR/RXR activation [*PRKCA*]) and oxidative stress (NRF-2-mediated oxidative response stress response (*GSTK1*) (table 4).

Pathways Unique to HC. The ingenuity pathway analysis identified six pathways for HC for positively correlated

Table 2. HCP Regions With Significant Morphometric Differences

HCP Region	Corresponding Brain Region	Cortical Thickness						Surface Area						Volume					
		FEAP Mean (sd)	HC Mean (sd)	F (d.f)	Sig (p)	% Change	Effect Size (d)	FEAP Mean (sd)	HC Mean (sd)	F (d.f)	Sig (p)	% Change	Effect Size (d)	FEAP Mean (sd)	HC mean (sd)	F (d.f)	Sig (p)	% change	Effect size (d)
Alterations in surface area and volume																			
Left area V3B	Dorsal stream visual cortex	—	—	—	—	—	—	213.22 (50.28)	225.94 (57.86)	4.20 (1)	0.04	−5.63%	−0.01	379.82 (113.73)	401.81 (118.93)	3.96 (1)	0.048	−5.79%	−0.003
Left medial area 7A	Superior parietal cortex	—	—	—	—	—	—	467.47 (104.47)	487.48 (105.80)	4.09 (1)	0.04	−4.28%	−0.003	1390.32 (283.69)	1442.88 (353.59)	7.29 (1)	0.008	−3.78%	−0.001
Left area 45	Inferior frontal cortex	—	—	—	—	—	—	596.48 (121.72)	548.41 (100.68)	6.15 (1)	0.01	8.06%	0.01	2055.55 (457.86)	1875.11 (396.01)	4.71 (1)	0.031	8.78%	0.002
Left superior 6-8 transitional alrea	Dorsolateral prefrontal cortex	—	—	—	—	—	—	242.86 (51.48)	251.54 (42.52)	4.47 (1)	0.04	−3.57%	−0.01	807.21 (238.71)	879.58 (229.81)	7.92 (1)	0.006	−8.97%	−0.003
Left area intra parietal 1	Inferior parietal cortex	—	—	—	—	—	—	521.02 (93.45)	539.36 (90.19)	4.27 (1)	0.04	−3.52%	−0.004	1340.71 (377.16)	1413.91 (388.61)	4.87 (1)	0.029	−5.46%	−0.001
Left area PGs	Inferior parietal cortex	—	—	—	—	—	—	944.16 (169.96)	987.26 (154.80)	6.49 (1)	0.01	−4.56%	−0.003	2943.69 (541.01)	3193.73 (522.86)	16.46 (1)	<.001	−8.49%	−0.002
Right area TE1 middle	Lateral temporal cortex	—	—	—	—	—	—	479.92 (90.42)	500.52 (83.55)	8.54 (1)	0.004	−4.29%	−0.006	1527.51 (398.20)	1656.59 (351.91)	11.61 (1)	<.001	−8.45%	−0.002
Alterations in cortical thickness and volume																			
Left area 5m ventral	Paracentral lobular and mid cingulate cortex	2.25 (0.16)	2.32 (0.16)	8.81 (1)	0.003	−3.11%	−0.41	—	—	—	—	—	—	719.53 (121.06)	741.15 (101.35)	4.76 (1)	0.031	−3.00%	−0.04
Left area 47s	Orbital and polar frontal cortex	3.02 (0.32)	3.12 (0.33)	5.57 (1)	0.019	−3.97%	−0.28	—	—	—	—	—	—	1332.73 (268.54)	1352.95 (224.90)	6.41 (1)	0.012	−1.52%	−0.001
Left inferior 6-8 transitional area	Dorsolateral prefrontal cortex	2.61 (0.22)	2.73 (0.24)	10.5 (1)	0.001	−4.60%	−0.52	—	—	—	—	—	—	1075.75 (254.78)	1177.11 (315.81)	9.94 (1)	0.002	−9.42%	−0.002
Left area TE1 posterior	Lateral temporal cortex	2.67 (0.22)	2.76 (0.22)	5.23 (1)	0.023	−3.37%	−0.35	—	—	—	—	—	—	3424.82 (607.53)	3535.74 (569.75)	7.93 (1)	0.005	−3.24%	−0.001
Left area anterior 32 prime	Anterior cingulate and medial prefrontal cortex	2.75 (0.19)	2.84 (0.20)	9.23 (1)	0.003	−3.27%	−0.42	—	—	—	—	—	—	908.69 (260.90)	966.58 (242.21)	6.59 (1)	0.011	−6.37%	−0.002
Right Inferior 6–8 transitional area	Dorsolateral prefrontal cortex	2.69 (0.26)	2.80 (0.24)	4.52 (1)	0.035	−4.09%	−0.36	—	—	—	—	—	—	1192 (298.65)	1243.75 (268.61)	4.76 (1)	0.031	−4.34%	−0.001
Right area TE1 posterior	Lateral temporal cortex	2.66 (0.24)	2.75 (0.26)	4.47 (1)	0.036	−3.38%	−0.35	—	—	—	—	—	—	2926.66 (599.52)	3119.11 (557.83)	13.35 (1)	<.001	−6.58%	−0.001

Table 2. Continued

HCP Region	Corresponding Brain Region	Cortical Thickness						Surface Area						Volume					
		FEAP Mean (sd)	HC Mean (sd)	F (d.f)	Sig (p)	% Change	Effect Size (d)	FEAP Mean (sd)	HC Mean (sd)	F (d.f)	Sig (p)	% Change	Effect Size (d)	FEAP Mean (sd)	HC mean (sd)	F (d.f)	Sig (p)	% change	Effect size (d)
Alterations in Cortical Thickness Only																			
Left premotor eye field	Premotor cortex	2.54 (0.27)	2.63 (0.27)	5.17 (1)	0.024	−3.54%	−0.29	—	—	—	—	—	—	—	—	—	—	—	—
Left retroinsular cortex	Early auditory cortex	2.52 (0.15)	2.58 (0.18)	5.93 (1)	0.016	−2.38%	−0.32	—	—	—	—	—	—	—	—	—	—	—	—
Left prostriate cortex	Medial temporal cortex	2.22 (0.21)	2.30 (0.21)	8.41 (1)	0.004	−3.60%	−0.33	—	—	—	—	—	—	—	—	—	—	—	—
Left area PFm complex	Inferior parietal cortex	2.62 (0.20)	2.58 (0.17)	6.78 (1)	0.01	1.53%	0.16	—	—	—	—	—	—	—	—	—	—	—	—
Right frontal eye fields	Premotor cortex	2.39 (0.20)	2.50 (0.28)	4.23 (1)	0.041	−4.60%	−0.44	—	—	—	—	—	—	—	—	—	—	—	—
Right area lateral occipital 2	MT+ complex and neighboring visual areas	2.63 (0.28)	2.57 (0.31)	5.89 (1)	0.016	2.28%	0.21	—	—	—	—	—	—	—	—	—	—	—	—
Right area dorsal 32	Anterior cingulate and medial prefrontal cortex	3.00 (0.22)	2.92 (0.23)	9.14 (1)	0.003	2.67%	0.32	—	—	—	—	—	—	—	—	—	—	—	—
Right area 9-46d	Dorsolateral prefrontal cortex	2.53 (0.16)	2.49 (0.16)	7.20 (1)	0.008	1.58%	0.22	—	—	—	—	—	—	—	—	—	—	—	—
Right area anterior 10p	Orbital and polar frontal cortex	2.49 (0.25)	2.42 (0.22)	5.22 (1)	0.024	2.81%	0.28	—	—	—	—	—	—	—	—	—	—	—	—
Right area s32	Anterior cingulate and medial prefrontal cortex	2.52 (0.46)	2.37 (0.39)	5.90 (1)	0.016	5.60%	0.27	—	—	—	—	—	—	—	—	—	—	—	—
Alterations in Surface Area Only																			
Left parieto-occipital sulcus area 2	Posterior cingulate cortex	—	—	—	—	—	—	718.99 (116.26)	677.12 (108.55)	5.31 (1)	0.022	5.82%	0.01	—	—	—	—	—	—
Left area 8Ad	Dorsolateral prefrontal cortex	—	—	—	—	—	—	762.49 (152.71)	792.35 (133.34)	5.95 (1)	0.016	−3.92%	−0.003	—	—	—	—	—	—
Left area IFSp	Inferior frontal cortex	—	—	—	—	—	—	347.18 (79.94)	320.48 (64.48)	3.93 (1)	0.049	7.69%	0.01	—	—	—	—	—	—

Table 2. Continued

HCP Region	Corresponding Brain Region	Cortical Thickness						Surface Area						Volume					
		FEAP Mean (sd)	HC Mean (sd)	F (d.f)	Sig (p)	% Change	Effect Size (d)	FEAP Mean (sd)	HC Mean (sd)	F (d.f)	Sig (p)	% Change	Effect Size (d)	FEAP Mean (sd)	HC mean (sd)	F (d.f)	Sig (p)	% change	Effect size (d)
Left area 111	Orbital and polar frontal cortex	—	—	—	—	—	—	654.76 (94.63)	667.15 (71.11)	4.51 (1)	0.035	-1.89%	-0.004	—	—	—	—	—	—
Left frontal opercular area 1	Posterior opercular cortex	—	—	—	—	—	—	143.98 (26.45)	133.93 (20.61)	5.21 (1)	0.024	6.98%	0.04	—	—	—	—	—	—
Right lateral area 7A	Superior parietal cortex	—	—	—	—	—	—	462.02 (92.62)	429.79 (75.32)	5.03 (1)	0.026	6.98%	0.01	—	—	—	—	—	—
Right entorhinal cortex	Medial temporal cortex	—	—	—	—	—	—	253.06 (36.92)	240.01 (37.96)	4.22 (1)	0.042	5.16%	0.02	—	—	—	—	—	—
Right area temporo-parietooccipital junction 2	Temporo-parieto-occipital junction	—	—	—	—	—	—	473.2 (109.49)	436.11 (84.25)	4.15 (1)	0.043	7.84%	0.01	—	—	—	—	—	—
Right area PGi	Inferior parietal cortex	—	—	—	—	—	—	1087.76 (271.33)	980.31 (209.18)	5.58 (1)	0.019	9.88%	0.005	—	—	—	—	—	—
Alterations in Volume Only																			
Left superior frontal language area	Anterior cingulate and medial prefrontal cortex	—	—	—	—	—	—	—	—	—	—	—	—	1914.55 (440.73)	2009.36 (378.73)	8.90 (1)	0.003	−4.95%	−0.001
Left posterior cingulate visual area	Posterior cingulate cortex	—	—	—	—	—	—	—	—	—	—	—	—	1037.27 (295.30)	1095.33 (279.51)	5.55 (1)	0.02	−5.60%	−0.001
Left supplementary and cingulate eye field	Anterior cingulate and medial prefrontal cortex	—	—	—	—	—	—	—	—	—	—	—	—	1909.79 (347.99)	1955.6 (341.82)	5.00 (1)	0.027	−2.40%	−0.001
Left area 6m anterior	Paracentral lobular and mid cingulate cortex	—	—	—	—	—	—	—	—	—	—	—	—	1984.44 (458.42)	2095.83 (419.51)	6.58 (1)	0.011	−5.61%	−0.001
Left area 3a	Somatosensory and motor cortex	—	—	—	—	—	—	—	—	—	—	—	—	1149 (137.15)	1187.73 (126.47)	8.61 (1)	0.004	−3.37%	−0.005
Left ventral area 6	Premotor cortex	—	—	—	—	—	—	—	—	—	—	—	—	1001.69 (228.86)	1033.59 (194.19)	5.15 (1)	0.025	−3.18%	−0.002
Left area 47m	Orbital and polar frontal cortex	—	—	—	—	—	—	—	—	—	—	—	—	413.02 (100.42)	426.42 (89.56)	4.71 (1)	0.031	−3.24%	−0.003

Table 2. Continued

HCP Region	Corresponding Brain Region	Cortical Thickness						Surface Area						Volume					
		FEAP Mean (sd)	HC Mean (sd)	F (d.f)	Sig (p)	% Change	Effect Size (d)	FEAP Mean (sd)	HC Mean (sd)	F (d.f)	Sig (p)	% Change	Effect Size (d)	FEAP Mean (sd)	HC mean (sd)	F (d.f)	Sig (p)	% change	Effect size (d)
Left area 9 middle	Anterior cingulate and medial prefrontal cortex	—	—	—	—	—	—	—	—	—	—	—	—	3199.82 (542.38)	3238.15 (496.37)	7.47 (1)	0.007	−1.20%	−0.0003
Left area 8B lateral	Dorsolateral prefrontal cortex	—	—	—	—	—	—	—	—	—	—	—	—	1621.12 (325.06)	1664.04 (299.89)	4.96 (1)	0.027	−2.65%	−0.001
Left area 9 posterior	Dorsolateral prefrontal cortex	—	—	—	—	—	—	—	—	—	—	—	—	1709.75 (362.52)	1756.62 (367.90)	4.04 (1)	0.046	−2.74%	−0.001
Left area 52	Early auditory cortex	—	—	—	—	—	—	—	—	—	—	—	—	357.27 (51.49)	366.32 (67.95)	4.61 (1)	0.033	−2.53%	−0.004
Left area TG dorsal	Lateral temporal complex	—	—	—	—	—	—	—	—	—	—	—	—	5818.44 (824.03)	5939.26 (691.98)	7.10 (1)	0.009	−2.08%	−0.001
Left area PF complex	Posterior opercular cortex	—	—	—	—	—	—	—	—	—	—	—	—	2904.99 (620.69)	3000.41 (631.53)	5.15 (1)	0.025	−3.28%	−0.0005
Left parainsular area	Insular and frontal opercular cortex	—	—	—	—	—	—	—	—	—	—	—	—	507.28 (93.65)	518.11 (94.51)	4.35 (1)	0.039	−2.13%	−0.002
Right area 3a	Somatosensory and motor cortex	—	—	—	—	—	—	—	—	—	—	—	—	1124.29 (156.54)	1154.64 (162.10)	4.79 (1)	0.03	−2.70%	−0.002
Right area STGa	Auditory association cortex	—	—	—	—	—	—	—	—	—	—	—	—	1231.38 (222.95)	1248 (212.58)	4.65 (1)	0.033	−1.35%	−0.001
Right area TG dorsal	Lateral temporal complex	—	—	—	—	—	—	—	—	—	—	—	—	6248.39 (903.60)	6295.62 (848.78)	4.78 (1)	0.03	−0.76%	−0.0001
Right area TE2 posterior	Lateral temporal cortex	—	—	—	—	—	—	—	—	—	—	—	—	1669.76 (357.33)	1734.23 (354.29)	5.87 (1)	0.017	−3.86%	−0.001
Right area intraparietal 1	Inferior parietal cortex	—	—	—	—	—	—	—	—	—	—	—	—	1275.48 (381.55)	1335.72 (302.37)	4.35 (1)	0.039	−4.72%	−0.001
Right area V4t	MT+ complex and neighboring visual areas	—	—	—	—	—	—	—	—	—	—	—	—	564.65 (146.15)	593.56 (132.97)	5.84 (1)	0.017	−5.12%	−0.003

Table 3. Top 10% Significantly Correlated Genes With Cortical Thickness

Genes with Significant Correlations in Both FEAP and HC in CT				Genes with Significant Correlation Unique to FEAP in CT		Genes with Significant Correlation Unique to HC in CT	
Positively Correlated Genes (n = 391)	**Negatively Correlated Genes (n = 116)**	**Genes with Positive Correlation in FEAP and Negative Correlation in HC (n = 186)**	**Genes with Negative Correlation in FEAP and Positive Correlation in HC (n = 186)**	**Genes with Positive Correlation (n = 134)**	**Genes with Negative Correlation (n = 86)**	**Genes with Positive Correlation (n = 11)***	**Genes with Negative Correlation (n = 27)***
RasGEF domain family member 1C (*RASGEF1C*)	imprinted in Prader-Willi syndrome (*IPW*)	ALK and LTK ligand 2 (*ALKAL2*)	calmegin (*CLGN*)	actin alpha cardiac muscle 1 (*ACTC1*)	LDL receptor related protein 12 (*LRP12*)	leucine rich repeat neuronal 2 (*LRRN2*)	leucine rich repeat containing 34 (*LRRC34*)
SRY-box transcription factor 4 (*SOX4*)	complexin 1 (*CPLX1*)	achaete-scute family bHLH transcription factor 2 (*ASCL2*)	FAST kinase domains 1 (*FASTKD1*)	atypical chemokine receptor 3 (*ACKR3*)	Pim-3 proto-oncogene, serine/threonine kinase (*PIM3*)	hydroxysteroid 17-beta dehydrogenase 10 (*HSD17B10*)	maestro heat like repeat family member 8 (*MROH8*)
G-protein subunit beta 4 (*GNB4*)	coiled-coil domain containing 39 (*CCDC39*)	prostaglandin E receptor 3 (*PTGER3*)	adenylate cyclase 9 (*ADCY9*)	synaptotagmin 10 (*SYT10*)	activin A receptor type 1C (*ACVR1C*)	potassium channel tetramerization domain containing 12 (*KCTD12*)	PIN2 (TERF1) interacting telomerase inhibitor 1 (*PINX1*)
adhesion molecule with Ig like domain 2 (*AMIGO*)	LDL receptor related protein associated protein 1 (*LRPAP1*)	neuropeptide Y receptor Y1 (*NPY1R*)	von Willebrand factor A domain containing 8 (*VWA8*)	S100 calcium binding protein A6 (*S100A6*)	solute carrier family 47 member 1 (*SLC47A1*)	CBLL1 antisense RNA 1 (*LOC101927974*)	HSPB1 associated protein 1 (*HSPBAP1*)
receptor transporter protein 1 (*RTP1*)	FAM20A golgi associated secretory pathway pseudokinase (*FAM20A*)	C3 and PZP like alpha-2-macroglobulin domain containing 8 (*CPAMD8*)	DND microRNA-mediated repression inhibitor 1 (*DND1*)	ALG1 like 1, pseudogene (*ALG1L*)	complexin 2 (*CPLX2*)	sulfide quinone oxidoreductase (*SQOR*)	G-protein-coupled receptor 161 (*GPR161*)
troponin T1, slow skeletal type (*TNNT1*)	ELOVL fatty-acid elongase 4 (*ELOVL4*)	transcription elongation factor A3 (*TCEA3*)	methyltransferase like 24 (*METTL24*)	cms1 ribosomal small subunit homolog (*CMSS1*)	coiled-coil domain containing 136 (*CCDC136*)		
scavenger receptor class A member 5 (*SCARA5*)	leucine rich repeat containing 37 member A4, pseudogene (*LRRC37A4P*)	signal peptide peptidase like 3 (*SPPL3*)	solute carrier family 16 member 6 (*SLC16A6*)	complement C1q A chain (*C1QA*)	synapsin III (*SYN3*)		
pterin-4 alpha-carbinolamine dehydratase 1 (*PCBD1*)	transmembrane protein 229B (*TMEM229B*)	prostaglandin E receptor 4 (*PTGER4*)	ectonucleoside triphosphate diphosphohydrolase 4 (*ENTPD4*)	N-sulfoglucosamine sulfohydrolase (*SGSH*)	abhydrolase domain containing 12, lysophospholipase (*ABHD12*)		
TAFA chemokine like family member 1 (*FAM19A1*)	Lysophosphatidylcholine acyltransferase 4 (*LPCAT4*)	NSFL1 cofactor (*NSFL1C*)	disheveled binding antagonist of beta catenin 2 (*DACT2*)	lysyl oxidase like 1 (*LOXL1*)	ceramide kinase (*CERK*)		
mitochondrial calcium uniporter dominant negative subunit beta (*MCUB*)	ubiquitin specific peptidase 45 (*USP45*)	TOX high mobility group box family member 3 (*TOX3*)	estrogen related receptor gamma (*ESRRG*)	phospholipase C eta 1 (*PLCH1*)			

Table 3. Continued

Genes with Significant Correlations in Both FEAP and HC in CT				Genes with Significant Correlation Unique to FEAP in CT		Genes with Significant Correlation Unique to HC in CT	
Positively Correlated Genes (n = 391)	**Negatively Correlated Genes (n = 116)**	**Genes with Positive Correlation in FEAP and Negative Correlation in HC (n = 186)**	**Genes with Negative Correlation in FEAP and Positive Correlation in HC (n = 186)**	**Genes with Positive Correlation (n = 134)**	**Genes with Negative Correlation (n = 86)**	**Genes with Positive Correlation (n = 11)***	**Genes with Negative Correlation (n = 27)***
EMG1 N1-specific pseudouridine methyltransferase (*EMG1*)	ubiquitin related modifier 1 (*URM1*)	copine 7 (*CPNE7*)	synaptotagmin 2 (*SYT2*)	metallothionein 1G (*MT1G*)			
receptor interacting serine/threonine kinase 2 (*RIPK2*)	glycerophosphocholine phosphodiesterase 1 (*GPCPD1*)	solute carrier family 7 member 4 (*SLC7A4*)	Bardet-Biedl syndrome 7 (*BBS7*)	FXYD domain containing ion transport regulator 6 (*FXYD6*)			
protocadherin 20 (*PCDH20*)		calcium and integrin binding 1 (*CIB1*)	beta-carotene oxygenase 2 (*BCO2*)	metallothionein 1X (*MT1X*)			
complement factor D (*CFD*)		Rab interacting lysosomal protein like 2 (*RILPL2*)	family with sequence similarity 222 member B (*FAM222B*)				
kelch domain containing 8B (*KLHDC8B*)		RNA binding motif protein 8A (*RBM8A*)	endonuclease/exonuclease/phosphatase family domain containing 1 (*EEPD1*)				
catechol-O-methyltransferase domain containing 1 (*COMTD1*)		H2B clustered histone 12 (*HIST1H2BK*)	BEN domain containing 6 (*BEND6*)				
TCF3 fusion partner (*TFPT*)		Src like adaptor (*SLA*)	solute carrier family 25 member 37 (*SLC25A37*)				
caspase 1 (*CASP1*)		G-protein subunit gamma 4 (*GNG4*)	eukaryotic elongation factor 2 kinase (*EEF2K*)				
component of oligomeric golgi complex 5 (*COG5*)		5'-nucleotidase domain containing 2 (*NT5DC2*)	HPS1 biogenesis of lysosomal organelles complex 3 subunit 1 (*HPS1*)				
sorting nexin 7 (*SNX7*)							
centromere protein W (*CENPW*)							
BAI1 associated protein 3 (*BAIAP3*)							

Table 3. Continued

Genes with Significant Correlations in Both FEAP and HC in CT				Genes with Significant Correlation Unique to FEAP in CT		Genes with Significant Correlation Unique to HC in CT	
Positively Correlated Genes (n = 391)	**Negatively Correlated Genes (n = 116)**	**Genes with Positive Correlation in FEAP and Negative Correlation in HC (n = 186)**	**Genes with Negative Correlation in FEAP and Positive Correlation in HC (n = 186)**	**Genes with Positive Correlation (n = 134)**	**Genes with Negative Correlation (n = 86)**	**Genes with Positive Correlation (n = 11)***	**Genes with Negative Correlation (n = 27)***
lysyl oxidase like 3 (*LOXL3*)							
transmembrane protein 263 (*TMEM263*)							
LIM domain only 3 (*LMO3*)							
ribonuclease H2 subunit C (*RNASEH2C*)							
TINCR ubiquitin domain containing (*TINCR*)							
CD6 molecule (*CD6*)							
N-acetylglucosamine kinase (*NAGK*)							
MPV17 mitochondrial inner membrane protein like 2 (*MPV17L2*)							
CD63 molecule (*CD63*)							
C2 calcium dependent domain containing 4C (*C2CD4C*)							
long intergenic non-protein coding RNA 2716 (*DKFZp779M0652*)							
WD repeat domain 86 (*WDR86*)							
protein kinase C delta (*PRKCD*)							
glycine receptor alpha 3 (*GLRA3*)							
tripartite motif containing 27 (*TRIM27*)							
thymosin beta 10 (*TMSB10*)							
glycogen phosphorylase L (*PYGL*)							

*Top 5 correlated genes included instead due to small sample size.

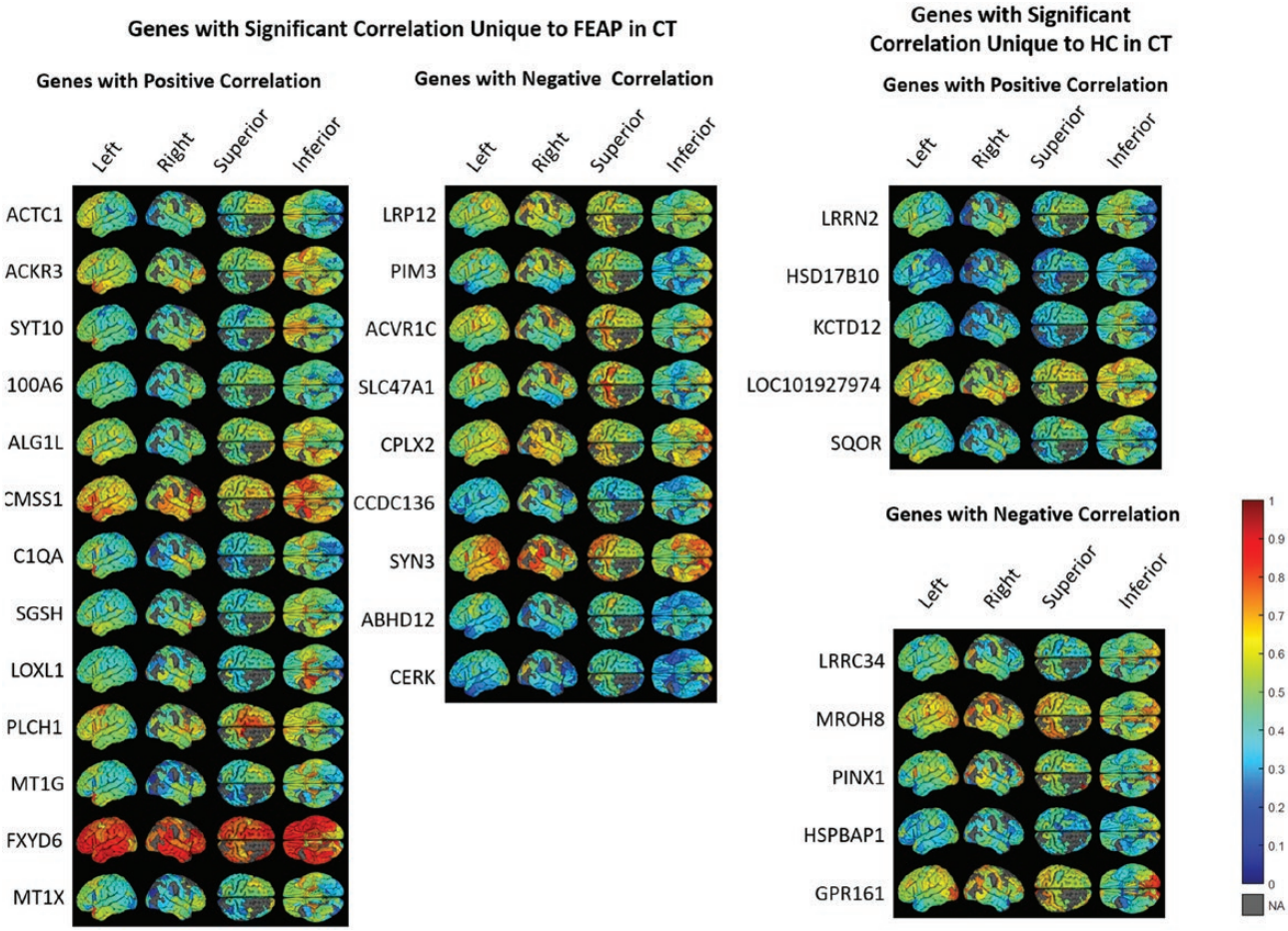

Fig 2. Heat map showing region-specific expression of top 10% of genes across the brain unique to FEAP and healthy controls with positive and negative correlations (Refer to table 3 for details).

gene expressions, e.g. Tryptophan Degradation III and Fatty-acid β oxidation I (*HSD17B10*), and 5 for negatively correlated genes, e.g. Methionine Degradation I (to Homocysteine) (*MAT2B*) and Telomere Extension by Telomerase (*PINX1*) (table 4).

Pathways Common Between FEAP and HC. The pattern of correlations of gene expressions with CT showed that there were 117 pathways from the 879 genes common to FEAP and HC. Fifty-five pathways were related to positively correlated gene expressions in both groups, e.g. synaptogenesis signaling pathway (*SCNA, PRKCD*), and 13 showed negative correlations in both groups, e.g. Calcium Transport I (*ATP2B2, ATP2B3*) and Myo-Inositol Biosynthesis (*INPP5F*). Forty-six pathways showed positive correlation among FEAP but negative correlation among controls, notably the Endocannabinoid Developing Neuron Pathway (*ADCY7, RAP2B*). Sixteen pathways showed negative correlation among FEAP but positive correlation among controls, e.g. Anandamide Degradation (*NAAA*) (table 4).

Pathways Among Schizophrenia and Non-schizophrenia: Seventy-nine pathways were identified for the 309 positively correlated genes among SZ patients, e.g. CXCR4 Signaling (*GNAQ*, *PLCB2*) and Synaptic Long-Term Depression (*IGF1*, *PLCD3*). Eleven pathways were significant among the 179 significantly negatively correlated genes in SZ patients, e.g. D-myo-inositol biosynthesis and metabolism (*DUSP8*, *SSH3*) and 3-phosphoinositide Degradation (*EYA4*, *PTPN2*). The only pathway that was significantly correlated with CT among NSZ was Telomere Extension by Telomerase (*PINX1*).

In summary, the SZ group had the most pathways associated with CT, while NSZ had the least number of identified pathways. Most pathways were identified for the positively correlated gene expressions compared to the negatively correlated ones.

Discussion

To the best of our knowledge, this is the first study employing "imaging transcriptomics" approach to comprehensively examine CT, SA, and GMV among FEAP. We report that the CT but not the SA or GMV of the brain regions significantly correlated with the expression of a small proportion of genes in both FEAP and

Table 4. Significant Ingenuity Pathway Analysis Pathways

Common for Both Groups	Direction of Correlation to Gene Expression	Genes	Unique to FEAP	Direction of Correlation to Gene Expression	Genes	Unique to HC	Direction of Correlation to Gene Expression	Genes
3-phosphoinositide biosynthesis	FEAP Positive, HC negative	*ACP1, NUDT2, PLPPR4, PPP1R1A, THTPA*	14-3-3-mediated signaling	Positive	*JUN, MAPK3, PLCH1*	Estrogen biosynthesis	Positive	*HSD17B13*
3-phosphoinositide degradation	FEAP positive, HC negative	*ACP1, NUDT2, PLPPR4, PPP1R1A, THTPA*	4-1BB signaling in T lymphocytes	Positive	*JUN, MAPK3*	Estrogen-dependent breast cancer signaling	Positive	*HSD17B14*
Antigen presentation pathway	FEAP positive, HC negative	*CANX, MR1*	Acute phase response signaling	Positive	*C1QA, C1QB, JUN, MAPK3*	Fatty-Acid β-oxidation I	Positive	*HSD17B10*
Antiproliferative role of somatostatin receptor 2	FEAP positive, HC negative	*GNG2, GNG4, RAP2B*	Agrin interactions at neuromuscular junction	Positive	*ACTC1, JUN, MAPK3*	Glutaryl-CoA degradation	Positive	*HSD17B11*
Apelin endothelial signaling pathway	FEAP positive, HC negative	*ADCY7, GNG2, GNG4, RAP2B*	BER (base excision repair) pathway	Positive	*MAPK3, RFC3*	Isoleucine degradation I	Positive	*HSD17B10*
Axonal guidance signaling	FEAP positive, HC negative	*ADAMTS9, EFNB2, GNG2, GNG4, NTNG2, PLCH2, RAP2B, SEMA4F, TUBB6*	cAMP-mediated signaling	Positive	*ADCY2, CNR1, MAPK3, OPRM1, RAPGEF4*	Tryptophan degradation III (eukaryotic)	Positive	*HSD17B12*
Breast cancer regulation by stathmin1	FEAP positive, HC negative	*ADGRF5, GNG2, GNG4, HGF, HTR1A, HTR7, NPY1R, PTGER3, PTGER4, RAP2B, SSTR1, TUBB6*	Chondroitin sulfate biosynthesis	Positive	*B3GALT6, CHST1*	Cysteine biosynthesis III (mammalia)	Negative	*MAT2B*
cAMP-mediated signaling	FEAP positive, HC negative	*ADCY7, HTR1A, HTR7, NPY1R, PKIA, PTGER3, PTGER4*	Colorectal cancer metastasis signaling	Positive	*ADCY2, JUN, MAPK3, SMAD2, WNT10B*	Methionine degradation I (to Homocysteine)	Negative	*MAT2B*
Cardiac β-adrenergic signaling	FEAP positive, HC negative	*ADCY7, GNG2, GNG4, PKIA, PPP1R1A*	Complement system	Positive	*C1QA, C1QB*	S-adenosyl-L-methionine biosynthesis	Negative	*MAT2B*
Catecholamine biosynthesis	FEAP positive, HC negative	*PNMT*	Corticotropin releasing hormone signaling	Positive	*ADCY2, CNR1, JUN, MAPK3*	Superpathway of methionine degradation	Negative	*MAT2B*
Colorectal cancer metastasis signaling	FEAP Positive, HC negative	*ADCY7, GNG2, GNG4, PTGER3, PTGER4, RAP2B*	Dermatan sulfate biosynthesis	Positive	*B3GALT6, CHST1*	Telomere extension by telomerase	Negative	*PINX1*
CREB signaling in neurons	FEAP positive, HC negative	*ADCY7, ADGRF5, GNG2, GNG4, HGF, HTR1A, HTR7, NPY1R, PLCH2, PTGER3, PTGER4, RAP2B, SSTR1*	EGF signaling	Positive	*JUN, MAPK3*			
D-myo-inositol (1,4,5,6)-tetrakisphosphate biosynthesis	FEAP positive, HC negative	*ACP1, NUDT2, PLPPR4, PPP1R1A, THTPA*	EIF2 signaling	Positive	*ACTC1, MAPK3, RPL27, RPL29, RPL36, RPS18*			

Table 4. Continued

Common for Both Groups	Direction of Correlation to Gene Expression	Genes	Unique to FEAP	Direction of Correlation to Gene Expression	Genes	Unique to HC	Direction of Correlation to Gene Expression	Genes
D-myo-inositol (3,4,5,6)-tetrakisphosphate biosynthesis	FEAP positive, HC negative	*ACP1, NUDT2, PLPPR4, PPP1R1A, THTPA*	Endocannabinoid developing neuron pathway	Positive	*ADCY2, CNR1, MAPK3*			
D-myo-inositol-5-phosphate metabolism	FEAP positive, HC negative	*ACP1, NUDT2, PLCH2, PLPPR4, PPP1R1A, THTPA*	Endocannabinoid neuronal synapse pathway	Positive	*ADCY2, CNR1, MAPK3, PLCH1*			
Endocannabinoid developing neuron pathway	FEAP positive, HC negative	*ADCY7, GNG2, GNG4, RAP2B*	Endothelin-1 signaling	Positive	*ADCY2, JUN, MAPK3, PLCH1*			
Endocannabinoid neuronal synapse pathway	FEAP positive, HC negative	*ADCY7, GNG2, GNG4, PLCH2*	FAT10 cancer signaling pathway	Positive	*ACKR3, SMAD2*			
Ephrin B signaling	FEAP positive, HC negative	*ACP1, EFNB2, GNG2, GNG4*	FAT10 signaling pathway	Positive	*PSMA6, UBE2Z*			
Ephrin receptor signaling	FEAP positive, HC negative	*ACP1, EFNB2, GNG2, GNG4, RAP2B*	Ferroptosis signaling pathway	Positive	*AIFM2, FTH1, MAPK3*			
Eumelanin biosynthesis	FEAP positive, HC negative	*MIF*	Gap junction signaling	Positive	*ACTC1, ADCY2, MAPK3, PLCH1*			
Fatty-acid activation	FEAP positive, HC negative	*SLC27A3, SLC27A5*	Glycoaminoglycan-protein linkage region biosynthesis	Positive	*B3GALT6*			
Fatty-acid β-oxidation I	FEAP positive, HC negative	*SLC27A3, SLC27A5*	GPCR-mediated nutrient sensing in enteroendocrine cells	Positive	*ADCY2, PLCH1, RAPGEF4*			
G-protein-coupled receptor signaling	FEAP positive, HC negative	*ADCY7, ADGRF5, GNG2, GNG4, HTR1A, HTR7, NPY1R, PTGER3, PTGER4, RAP2B, SSTR1*	Gα12/13 signaling	Positive	*CDH9, JUN, MAPK3*			
GABA receptor signaling	FEAP positive, HC negative	*ADCY7, GNG2, GNG4, UBA52*	Gαi signaling	Positive	*ADCY2, CNR1, MAPK3, OPRM1*			
Gap junction signaling	FEAP positive, HC negative	*ADCY7, CCN3, PLCH2, RAP2B, TUBB6*	Hepatic fibrosis signaling pathway	Positive	*CCN2, CNR1, FTH1, JUN, MAPK3, SMAD2, WNT10B*			
Glutamate receptor signaling	FEAP positive, HC negative	*GNG2, GNG4, SLC1A6*	IGF-1 Signaling	Positive	*CCN2, JUN, MAPK3*			

Table 4. Continued

Common for Both Groups	Direction of Correlation to Gene Expression	Genes	Unique to FEAP	Direction of Correlation to Gene Expression	Genes	Unique to HC	Direction of Correlation to Gene Expression	Genes
GPCR-mediated nutrient sensing in enteroendocrine cells	FEAP positive, HC negative	*ADCY7, GNG2, GNG4, PLCH2*	IL-17A signaling in Fibroblasts	Positive	*JUN, MAPK3*			
Gαi signaling	FEAP positive, HC negative	*ADCY7, GNG2, GNG4, HTR1A, NPY1R, PTGER3, RAP2B*	IL-17A signaling in gastric cells	Positive	*JUN, MAPK3*			
Gαs signaling	FEAP positive, HC negative	*ADCY7, GNG2, GNG4, HTR7, PTGER4*	Iron homeostasis signaling pathway	Positive	*FTH1, MAPK3, SMAD2*			
IL-1 signaling	FEAP positive, HC negative	*ADCY7, GNG2, GNG4*	JAK/STAT signaling	Positive	*JUN, MAPK3, PIAS3*			
LPS/IL-1 mediated inhibition of RXR function	FEAP positive, HC negative	*FABP7, HMGCS1, MGMT, SLC27A3, SLC27A5*	Leptin signaling in obesity	Positive	*ADCY2, MAPK3, PLCH1*			
Methylglyoxal degradation VI	FEAP positive, HC negative	*LDHD*	Mechanisms of viral exit from host cells	Positive	*ACTC1, CHMP2A*			
Mitochondrial L-carnitine shuttle pathway	FEAP positive, HC negative	*SLC27A3, SLC27A6*	MIF regulation of innate immunity	Positive	*JUN, MAPK3*			
Myo-inositol biosynthesis	FEAP positive, HC negative	*ISYNA1*	NADH repair	Positive	*NAXE*			
Notch signaling	FEAP positive, HC negative	*CNTN1, DLL3*	NRF2-mediated oxidative stress response	Positive	*ACTC1, FTH1, JUN, MAPK3, PRDX1*			
P2Y purigenic receptor signaling pathway	FEAP positive, HC negative	*ADCY7, GNG2, GNG4, PLCH2, RAP2B*	P2Y purigenic receptor signaling pathway	Positive	*ADCY2, JUN, MAPK3, P2RY6, PLCH1*			
Prolactin signaling	FEAP positive, HC negative	*KCNMB2, KCNMB4, RAP2B*	Polyamine regulation in colon cancer	Positive	*JUN, MAPK3*			
Renal cell carcinoma signaling	FEAP positive, HC negative	*HGF, RAP2B, UBA52*	PPARα/RXRα activation	Positive	*ADCY2, JUN, MAPK3, PLCH1, SMAD2*			
Role of NFAT in cardiac hypertrophy	FEAP positive, HC negative	*ADCY7, GNG2, GNG4, PLCH2, RAP2B*	Pulmonary fibrosis idiopathic signaling pathway	Positive	*ACTC1, CCN2, COL23A1, JUN, MAPK3, SMAD2, WNT10B*			
Serotonin receptor signaling	FEAP positive, HC negative	*ADCY7, HTR1A, HTR7*	RAR activation	Positive	*ADCY2, DHRS9, JUN, SMAD2*			

Table 4. Continued

Common for Both Groups	Direction of Correlation to Gene Expression	Genes	Unique to FEAP	Direction of Correlation to Gene Expression	Genes	Unique to HC	Direction of Correlation to Gene Expression	Genes
Stearate biosynthesis I (Animals)	FEAP positive, HC negative	*ACOT2, SLC27A3, SLC27A5*	Renin-angiotensin signaling	Positive	*ADCY2, JUN, MAPK3*			
Superpathway of cholesterol biosynthesis	FEAP positive, HC negative	*DHCR7, HMGCS1*	Sphingosine-1-phosphate signaling	Positive	*ADCY2, MAPK3, PLCH1*			
Superpathway of inositol phosphate compounds	FEAP positive, HC negative	*ACP1, NUDT2, PLCH2, PLPPR4, PPP1R1A, THTPA*	SPINK1 general cancer pathway	Positive	*MAPK3, MT1B, MT1E, MT1F, MT1G, MT1X*			
Thrombin signaling	FEAP positive, HC negative	*ADCY7, GNG2, GNG4, PLCH2, RAP2B*	Sumoylation pathway	Positive	*JUN, RFC3, SUMO2*			
α-Adrenergic signaling	FEAP positive, HC negative	*ADCY7, GNG2, GNG4, RAP2B*	Synaptogenesis signaling pathway	Positive	*gADCY2, CDH9, MAPK3, MARCKS, SYT10*			
γ-linolenate biosynthesis II (animals)	FEAP positive, HC negative	*SLC27A3, SLC27A5*	TGF-β signaling	Positive	*JUN, MAPK3, SMAD2*			
Anandamide degradation	FEAP negative, HC positive	*NAAA*	UVA-induced MAPK signaling	Positive	*JUN, MAPK3, PLCH1*			
Aryl hydrocarbon receptor signaling	FEAP negative, HC positive	*ALDH1A3, NCOA3, NFIC, TNF, TRIP11*	UVB-induced MAPK signaling	Positive	*JUN, MAPK3*			
CDP-diacylglycerol biosynthesis I	FEAP negative, HC positive	*CDS1, GPAT3*	UVC-induced MAPK signaling	Positive	*JUN, MAPK4*			
Creatine-phosphate biosynthesis	FEAP negative, HC positive	*CKMT1A/CKMT1B*	Actin nucleation by ARP-WASP complex	Negative	*RHOBTB2, ROCK2*			
CXCR4 signaling	FEAP negative, HC positive	*ADCY9, ELMO3, PIK3CA, RHOQ*	Cardiac hypertrophy signaling (Enhanced)	Negative	*ACVR1C, AKAP13, FGF7, PDE4A, PRKCA, ROCK2*			
FAT10 signaling Pathway	FEAP negative, HC positive	*MAP1LC3B, NUB1, TNF*	Chemokine signaling	Negative	*PRKCA, ROCK2*			
Fatty-acid α-oxidation	FEAP negative, HC positive	*ALDH1A3, BCO2*	Cholecystokinin/ Gastrin-mediated signaling	Negative	*PRKCA, RHOBTB2, ROCK2*			
Germ cell-sertoli cell junction signaling	FEAP negative, HC positive	*PIK3CA, RHOQ, SORBS1, TNF*	CXCR4 signaling	Negative	*PRKCA, RHOBTB2, ROCK2*			
IL-9 signaling	FEAP negative, HC positive	*PIK3CA, TNF*	Factors promoting cardiogenesis in vertebrates	Negative	*ACVR1C, PRKCA, ROCK2*			

Table 4. Continued

Common for Both Groups	Direction of Correlation to Gene Expression	Genes	Unique to FEAP	Direction of Correlation to Gene Expression	Genes	Unique to HC	Direction of Correlation to Gene Expression	Genes
LPS/IL-1 mediated inhibition of RXR function	FEAP negative, HC positive	*ACSL6, ALDH1A3, HS3ST1, PPARGC1A, TNF*	FGF signaling	Negative	*FGF7, PRKCA*			
p38 MAPK signaling	FEAP negative, HC positive	*EEF2K, MAX, TIFA, TNF*	Gαq signaling	Negative	*PRKCA, RHOBTB2, ROCK2*			
Phosphatidylglycerol biosynthesis II (non-plastidic)	FEAP negative, HC positive	*CDS1, GPAT3*	Hepatic fibrosis signaling pathway	Negative	*ACVR1C, GLIS1, PRKCA, RHOBTB2, ROCK2*			
Role of hypercytokinemia/ hyperchemokinemia in the pathogenesis of influenza	FEAP negative, HC positive	*IFNLR1, MX1, TNF*	IL-8 signaling	Negative	*PRKCA, RHOBTB2, ROCK2*			
S-methyl-5'-thioadenosine degradation II	FEAP negative, HC positive	*MTAP*	Lysine degradation II	Negative	*AASDH*			
Sphingosine-1-phosphate signaling	FEAP negative, HC Positive	*ADCY9, NAAA, PIK3CA, RHOQ*	Lysine degradation V	Negative	*AASDH*			
TR/RXR activation	FEAP negative, HC positive	*NCOA3, PIK3CA, PPARGC1A, SYT2*	NRF2-mediated oxidative stress response	Negative	*DNAJC4, FKBP5, GSTK1, PRKCA*			
14-3-3-mediated signaling	FEAP and HC positive	*PRKCD, RRAS2, SNCA, TUBB2A, TUBB4B, YWHAH*	RHOGDI signaling	Negative	*PRKCA, RHOBTB2, ROCK2*			
Adipogenesis pathway	FEAP and HC positive	*CEBPA, ERCC2, FZD2, FZD8, FZD9, GTF2H5*	Semaphorin signaling in neurons	Negative	*RHOBTB2, ROCK2*			
AMPK signaling	FEAP and HC positive	*ADRA1B, ADRA2C, EIF4EBP1, GNB2, GNB4, HMGCR, MAPK11, PPM1M, SMARCD3*	VDR/RXR activation	Negative	*PPARD, PRKCA*			
Amyotrophic lateral sclerosis signaling	feap and hc positive	*BIRC3, CASP1, GRID2, GRIN3A, IGF1, PDGFC, SSR4*						
Androgen signaling	FEAP and HC positive	*ERCC2, GNB2, GNB4, GTF2H5, POLR2G, POLR2L, PRKCD, SHC1, TAF10*						
Antiproliferative role of somatostatin receptor 2	FEAP and HC positive	*GNB2, GNB4, RRAS2, SST*						

Table 4. Continued

Common for Both Groups	Direction of Correlation to Gene Expression	Genes	Unique to FEAP	Direction of Correlation to Gene Expression	Genes	Unique to HC	Direction of Correlation to Gene Expression	Genes
Assembly of RNA polymerase II complex	FEAP and HC positive	*ERCC2, GTF2H5, POLR2G, POLR2L, TAF10*						
Axonal guidance signaling	FEAP and HC positive	*ARPC2, CHMP1A, FZD2, FZD8, FZD9, GNB2, GNB4, IGF1, MYL12B, PDGFC, PRKCD, RRAS2, SHC1, SLIT1, TUBB2A, TUBB4B*						
Breast cancer regulation by stathmin1	FEAP and HC positive	*ADGRB3, ADRA1B, ADRA2C, FZD2, FZD8, FZD9, GNB2, GNB4, GPR68, GPR88, IGF1, NTSR1, OPRK1, PDGFC, PRKCD, RRAS2, SHC1, TUBB2A, TUBB4B*						
Cardiac hypertrophy signaling	FEAP and HC positive	*ADRA1B, ADRA2C, GNB2, GNB4, HSPB1, IGF1, MAPK11, MYL12B, RRAS2*						
Cardiac Hypertrophy signaling (enhanced)	FEAP and HC positive	*ADRA1B, ADRA2C, EDN1, EIF4EBP1, FZD2, FZD8, FZD9, GNB2, GNB4, HSPB1, IGF1, IL13RA2, MAPK11, NPPA, PRKCD, RRAS2, TG*						
Cholesterol biosynthesis I	FEAP and HC positive	*FDFT1, MSMO1, TM7SF2*						
Cholesterol biosynthesis II (via 24,25-dihydrolanosterol)	FEAP and HC positive	*FDFT1, MSMO1, TM7SF2*						
Cholesterol biosynthesis III (via desmosterol)	FEAP and HC positive	*FDFT1, MSMO1, TM7SF2*						
CLEAR signaling pathway	FEAP and HC positive	*ATP6V1C1, CD63, IGF1, LAMTOR2, MAPK11, PDGFRA, PRKCD, RRAS2, SCPEP1, TNFRSF11A, YWHAH*						
CREB signaling in neurons	FEAP and HC positive	*ADGRB3, ADRA1B, ADRA2C, FZD2, FZD8, FZD9, GNB2, GNB4, GPR68, GPR88, GRID2, IGF1, NTSR1, OPRK1, PDGFRA, POLR2G, POLR2L, PRKCD, RRAS2, SHC1, TNFRSF11A*						
Endothelin-1 signaling	FEAP and HC positive	*CASP1, EDN1, MAPK11, PLAAT1, PNPLA3, PRKCD, RRAS2, SHC1*						

Table 4. Continued

Common for Both Groups	Direction of Correlation to Gene Expression	Genes	Unique to FEAP	Direction of Correlation to Gene Expression	Genes	Unique to HC	Direction of Correlation to Gene Expression	Genes
Ephrin receptor signaling	FEAP and HC Positive	*ARPC2, DOK1, GNB2, GNB4, GRIN3A, PDGFC, RRAS2, SHC1*						
Epoxysqualene biosynthesis	FEAP and HC positive	*FDFT1*						
ERBB signaling	FEAP and HC positive	*BTC, MAPK11, PRKCD, RRAS2, SHC1*						
ERBB4 signaling	FEAP and HC positive	*PRKCD, PSENEN, RRAS2, SHC1*						
G-protein-coupled receptor signaling	FEAP and HC positive	*ADGRB3, ADRA1B, ADRA2C, FZD2, FZD8, FZD9, GNB2, GNB4, GPR68, GPR88, GPRIN1, HCN4, MAPK11, MYL12B, NTSR1, OPRK1, RGS10, RRAS2, SHC1*						
Glioblastoma multiforme signaling	FEAP and HC positive	*FZD2, FZD8, FZD9, IGF1, PDGFC, PDGFRA, PRKCD, RRAS2, SHC1*						
Glioma signaling	FEAP and HC positive	*CDKN2D, IGF1, PDGFC, PDGFRA, PRKCD, RRAS2, SHC1*						
Glucocorticoid receptor signaling	FEAP and HC positive	*ANXA1, ATP5MC1, CEBPA, DNALI1, ERCC2, GTF2H5, IGF1, IL13RA2, KRT86, MAPK11, NPPA, POLR2G, POLR2L, RRAS2, SHC1, SMARCD3, TAF10, YWHAH*						
Glutamate receptor signaling	FEAP and HC positive	*GNB2, GNB4, GRID2, GRIN3A, SLC17A8*						
Gαi signaling	FEAP and HC positive	*ADRA2C, GNB2, GNB4, OPRK1, RGS10, RRAS2, SHC1*						
Hepatic fibrosis/ hepatic stellate cell activation	FEAP and HC positive	*COL21A1, EDN1, IGF1, KLF6, LAMA1, PDGFC, PDGFRA*						
Histamine biosynthesis	FEAP and HC positive	*HDC*						
Human embryonic stem cell pluripotency	FEAP and HC positive	*FZD2, FZD8, FZD9, GNB2, GNB4, PDGFC, PDGFRA*						
Huntington's disease signaling	FEAP and HC positive	*ATP5MC1, CASP1, GNB2, GNB4, IGF1, POLR2G, POLR2L, PRKCD, PSMB1, PSMB6, SHC1, SNCA, STX1A*						
Inflammasome pathway	FEAP and HC positive	*CASP1, PYCARD*						

Table 4. Continued

Common for Both Groups	Direction of Correlation to Gene Expression	Genes	Unique to FEAP	Direction of Correlation to Gene Expression	Genes	Unique to HC	Direction of Correlation to Gene Expression	Genes
Intrinsic prothrombin activation pathway	FEAP and HC positive	*KLK10, KLK5, KLK7*						
L-glutamine biosynthesis II (tRNA-dependent)	FEAP and HC positive	*GATB*						
Mevalonate pathway I	FEAP and HC positive	*HMGCR, PMVK*						
Molecular mechanisms of cancer	FEAP and HC positive	*BIRC3, CDK17, CDKN2D, FZD2, FZD8, FZD9, GNB2, GNB4, MAPK11, PRKCD, PSENEN, RRAS2, SHC1*						
Mouse embryonic stem cell pluripotency	FEAP and HC positive	*FZD2, FZD8, FZD9, MAPK11, RRAS2*						
MSP-RON signaling in cancer cells pathway	FEAP and HC positive	*KLK10, KLK5, KLK7, PDGFC, RRAS2, YWHAH*						
NER (nucleotide excision repair, enhanced pathway)	FEAP and HC positive	*CETN2, ERCC2, GTF2H5, POLE4, POLR2G, POLR2L*						
Neuroinflammation signaling pathway	FEAP and HC positive	*BIRC3, CASP1, GABRA3, GABRA5, GABRE, GRIN3A, MAPK11, PSENEN, PYCARD, SNCA*						
Neuroprotective role of THOP1 in alzheimer's disease	FEAP and HC positive	*C1R, CFD, KLK10, KLK5, KLK7, SST*						
Nucleotide excision repair pathway	FEAP and HC positive	*ERCC2, GTF2H5, POLR2G, POLR2L*						
Oxytocin in brain signaling pathway	FEAP and HC positive	*CASP1, GNB2, GNB4, PLAAT1, PNPLA3, PRKCD, PYCARD, RRAS2*						
Parkinson's signaling	FEAP and HC positive	*MAPK11, SNCA*						
RHOGDI signaling	FEAP and HC positive	*ARHGDIG, ARPC2, CDH10, CDH11, CDH13, GNB2, GNB4, MYL12B*						
Role of MAPK signaling in promoting the pathogenesis of influenza	FEAP and HC positive	*ATP6V1C1, MAPK11, PLAAT1, PNPLA3, RRAS2*						

Table 4. Continued

Common for Both Groups	Direction of Correlation to Gene Expression	Genes	Unique to FEAP	Direction of Correlation to Gene Expression	Genes	Unique to HC	Direction of Correlation to Gene Expression	Genes
Role of MAPK signaling in the pathogenesis of influenza	FEAP and HC positive	*MAPK11, PLAAT1, PNPLA3, RRAS2*						
STAT3 pathway	FEAP and HC positive	*IGF1, IL13RA2, MAPK11, PDGFRA, RRAS2, TNFRSF11A*						
Superpathway of cholesterol Biosynthesis	FEAP and HC positive	*FDFT1, FDPS, HMGCR, MSMO1, PMVK, TM7SF2*						
Superpathway of Geranylgeranyldiphosphate Biosynthesis I (via Mevalonate)	FEAP and HC positive	*FDPS, HMGCR, PMVK*						
Synaptic long-term depression	FEAP and HC positive	*GRID2, IGF1, PLAAT1, PNPLA3, PPP1R17, PRKCD, RRAS2*						
Synaptogenesis signaling pathway	FEAP and HC positive	*ARPC2, CDH10, CDH11, CDH13, CPLX3, EIF4EBP1, GRIN3A, PRKCD, RRAS2, SHC1, SNCA, STX1A, SYT17*						
Thrombin signaling	FEAP and HC positive	*ARHGEF28, GNB2, GNB4, MAPK11, MYL12B, PRKCD, RRAS2, SHC1*						
Zymosterol biosynthesis	FEAP and HC positive	*MSMO1, TM7SF2*						
α-Adrenergic signaling	FEAP and HC positive	*GNB2, GNB4, PRKCD, PYGL, RRAS2*						
1D-myo-inositol hexakisphosphate biosynthesis II (mammalian)	FEAP and HC negative	*INPP5A, INPP5F*						
Calcium transport I	FEAP and HC negative	*ATP2B2, ATP2B3*						
Chondroitin sulfate biosynthesis	FEAP and HC negative	*HS6ST2, XYLT2*						
D-myo-inositol (1,3,4)-trisphosphate Biosynthesis	FEAP and HC negative	*INPP5A, INPP5F*						
D-myo-inositol (1,4,5)-trisphosphate Degradation	FEAP and HC negative	*INPP5A, INPP5F*						
Dermatan sulfate biosynthesis	FEAP and HC negative	*HS6ST2, XYLT2*						

Table 4. Continued

Common for Both Groups	Direction of Correlation to Gene Expression	Genes	Unique to FEAP	Direction of Correlation to Gene Expression	Genes	Unique to HC	Direction of Correlation to Gene Expression	Genes
Glycoaminoglycan-protein linkage region biosynthesis	FEAP and HC negative	*XYLT2*						
Heparan sulfate biosynthesis	FEAP and HC negative	*HS6ST2, XYLT2*						
Myo-inositol biosynthesis	FEAP and HC negative	*INPP5F*						
Pyrimidine deoxyribonucleotides de novo biosynthesis I	FEAP and HC negative	*CMPK1, NME5*						
Pyrimidine ribonucleotides de novo biosynthesis	FEAP and HC negative	*CMPK1, NME5*						
Pyrimidine ribonucleotides interconversion	FEAP and HC negative	*CMPK1, NME5*						
Superpathway of D-myo-inositol (1,4,5)-trisphosphate Metabolism	FEAP and HC negative	*INPP5A, INPP5F*						

SZ, and even smaller proportion among NSZ using a standardized published pipeline which provides the most accurate gene expression dataset using the AHBA database.[33] Within this small proportion of genes whose expressions significantly correlated with CT, 10 had shown genome-wide association in the recent GWAS study.[46] Taking all transcripts correlated with CT, 17.5% more transcripts were among FEAP than HC, suggesting that CT in FEAP may be relatively highly genetically determined than SA or GMV. Within the FEAP group, association of higher number of gene expressions in SZ with CT compared to HC suggests that the CT in SZ may also be under greater genetic influence within FEAP, but NSZ with fewer unique gene expressions correlated with CT compared to HC suggests that the CT among NSZ may be under weaker genetic influence than among SZ. These findings suggest that expression of a small portion of genes may influence CT in both FEAP and SZ. Many unique pathways were associated with each group, e.g. selected inflammation-related pathways with FEAP, telomere extension with controls, and axonal guidance and sphingosine pathways with both groups. Overall, these observations suggest that sets of unique genes and pathways underlie variations in CT in FEAP and SZ providing targets for further elucidation of pathophysiological pathways and novel treatment approaches.

Our finding that CT but not SA or GMV significantly correlated with gene expression partly supported our hypotheses that morphometric features would show different patterns of correlations. Precise reasons for relative specificity of correlation with CT and lack of correlation with SA and GMV need further investigations. It is also unclear whether such correlations with CT are specific to the antipsychotic-naïve status of patients with short duration of illness where the confounds related to medication treatment and longer duration of illness are minimized. Future studies need to examine this issue since exposure to medications and attendant comorbidities may alter local gene expressions. A prior twin study reported globally and regionally high heritability of SA (0.89) and CT (0.81) but were only weakly correlated with each other[47] suggesting different genetic architecture of CT and SA. For example, heritability may be related to different cytoarchitectonic patterns because CT depends on the neuronal numbers and SA on the number of cortical columns[48] and possibly glial numbers.[49] A recent study reported correlation of CT with cell-specific gene expressions.[24] Among them, *FABP7* expressed in astrocytes was positively correlated with CT among FEAP and negatively among HC in our study. *FABP7* is significantly associated with lipopolysaccharide/Interleukin-1 (LPS/IL1)-mediated RXR function pathway. These data suggest that there are merit in examining the components of volume to better understand genetic architecture of morphometric features and elucidate potential impact of gene expression on underlying cytoarchitecture.

We predicted that the regions showing case–control differences would correlate with gene expressions, since disease-driven morphometric changes may be partly explained by the higher variance contributed by heritability than for regions that do not show case–control differences. Our findings did not support that prediction. A prior study focusing only on regions that showed group differences reported significant correlation of expression of several genes.[50] In our study, only a small proportion of regions (≈6%) showed altered morphometric features with small effect sizes among FEAP consistent with a recent study that compared first-episode antipsychotic-naïve SZ with multi-episode SZ and reported no cortical thinning in first-episode SZ.[51] In contrast, chronic medicated SZ[52] and early-onset adolescent SZ[53] subjects showed more widespread cortical thinning. In our previous study, we observed that CT and SA showed significant neurogenetic effects in the later phases of illness but not in the early phases.[54] We also observed that the genetic effects shared between deficits in general cognition and schizophrenia were nonsignificant in the early phases of the illness than during the later stages.[55] These data suggest that gene expression differences may impact CT changes in patients with longer duration of illness than those with short duration of illness. Since hundreds of gene expressions of small effects correlated with CT, multiple pathways may underlie such correlations. In addition to molecular pathways common to both FEAP and HC related to CT (e.g. axonal guidance signaling, synaptogenesis signaling, endocannabinoid developing neuron pathway), there were additional unique pathways associated with CT among FEAP, e.g., IL-1, IL-2, and IL-8 signaling, and complement pathways that may have affected CT. Since inflammation is related to cortical thinning,[56,57] other pathways regulating synaptogenesis signaling, neuronal number, or synapses might be modulating the observed CT in our study. Thus, overall case–control differences in CT may be determined by the stage of the illness, medication treatment, age at onset, a combination of environmental factors interacting with multiple genes[58,59] and interactions among different genes.[12,60]

Among the SZ risk genes reported in the recent GWAS study,[46] correlation of expression of *GRAMD1B, HYI, and MAPK3* that were unique to CT among FEAP are involved in the pathophysiology of SZ. *GRAMD1B,* located on chromosome 11q24.1, codes for endoplasmic reticulum proteins that enable phospholipid and cholesterol binding activity, which is important for regulation of various neuronal activities including energy uptake and metabolism, and neuronal membrane expansion during neuropil expansion. Similarly, the protein encoded by *HYI,* located on 1q34.2, is involved in carbohydrate metabolism. *MAPK3* codes for a protein in the MAPK family that participates in cellular activities such as differentiation, proliferation, and cell cycle progression. Prior studies suggest that some of these

pathways were associated with SZ. For example, altered cerebral bioenergetics is supported by convergent data that shows the association of high energy phosphate metabolites with abnormal functional connectivity,[61] changes in neurotransmitters such as glutamate,[62] cognitive impairments,[63] hallucinations,[64] and overall severity of psychopathology.[65,66] These mechanisms may underlie cortical thinning in observed regions, but precise pathways need to be elucidated in future studies.

Seven GWAS genes that were common to both FEAP and controls (*ENOX1, KANSL1, KLF 6, MLXIP, PLCH2, RNASEH2C,* and *FAM216A)* participate in molecular pathways of interest to SZ. Some of them are electron transport pathway[67,68] (*ENOX1*), histone acetylation[69,70] (*KANSL1*), tumor suppressor activity[71] (*KLF 6*), regulation of genes in response to cellular glucose levels[72] (*MLXIP*), cleaving phosphatidyl inositol—a membrane phospholipid (MPL)—to generate second messengers such as inositol 1,4,5-triphosphate and diacylglycerol[73,74] (*PLCH2*). The latter gene is also involved in the formation and maintenance of neuronal networks in the postnatal brain. Association of pathways related to *RNASEH2C* (ribonuclease H2 subunit C) that cleaves ribonucleotide from RNA:DNA duplexes and *FAM216A* with SZ are not clear. Within this set of genes, 2 are related to cellular energy regulation while others are associated with inflammatory response, cell growth, and gene regulation. Some of these pathways have been associated with altered CT.[56,57] Thus, variants on these genes may contribute to pathophysiology through one of these pathways providing putative targets for further investigations.

Pathway analyses found association of some unique and overlapping molecular pathways with FEAP and HC, but more pathways were common to both groups suggesting that the gene expressions common to both groups may be relatively less important for pathophysiology of psychoses or SZ. In other words, analysis of genes associated with pathways unique to SZ may more likely highlight pathophysiologically significant molecular mechanisms contributing to CT in SZ, e.g. inflammation, oxidative stress, glutamate signaling, and serotonin signaling pathways. Some genes were associated with multiple pathways, e.g. dermatan sulfate involved in neuronal development, formation of neuronal network, and neuronal diversity.[75] Similarly, sphingosine pathway involving *NAAA* was associated with cortical atrophy,[76,77] regulation of neurite extension and neuronal plasticity[78] and metabolism of sphingolipids such as sphingomyelin found in the plasma membrane are involved in neurodevelopment.[79] In addition, multiple genes, e.g. *ACTC1*, *FTH1*, *MAPK3, PRDX1,* and *JUN* participated in the NRF2-mediated oxidative stress response pathway. Thus, our findings are consistent with observations that one gene may participate in multiple pathways and a given pathway may be affected by multiple genes. Pathways involving MPL metabolism (phosphatidylglycerol) and enzymes regulating the synthesis and catabolism of MPLs (phospholipases) were associated with CT. These findings concur with our prior studies using phosphorus magnetic resonance spectroscopy (^{31}P MRS) that showed altered MPL metabolism in SZ.[80–82] In addition, genes that were significantly correlated with CT are involved in the regulation of neurotransmitter secretion (e.g. glycine) and synaptic transmission (e.g. calcium ion channels, GABA). Further investigations would be necessary to elucidate differential effects and quantitively different levels of expression of such genes in controls, and persons with psychoses and to characterize unique effects of genes in these groups. While those that were unique to the disease could be the ones to follow-up for further characterization to understand pathophysiology and possibly to identify molecular targets for novel treatment design.

Our study has several strengths and innovative aspects. This is the first study, as far as we know, using imaging transcriptomics approach to concurrently examine 3 morphometric features among FEAP subjects, and SZ and NSZ subgroups. A recent study on first-episode schizophrenia used the coordinates of the regions observed in a meta-analysis to correlate with gene expression.[27] Although it is an interesting approach, our study used the direct measurement of 3 morphometric features to conduct correlations using a widely used analytical pipeline. A unique advantage of examining FEAP is that it minimizes the impact of medications and illness duration on the findings. We have examined FEAP consisting of different psychotic disorders in the spirit of Research Domain Criteria (RDoC) framework. Compared to prior studies correlating the AHBA's expression data[23,24] with Desikan–Killiany-Tourville-atlas-based 62 cortical ROIs[83] or voxel-based GMVs,[27] we utilized the HCP-atlas that defines 360 ROIs that used topography, anatomical and functional connectivity, function, and architecture for parcellations compared to other atlases that use one of these for mapping gene expression. The HCP-atlas was also parcellated by algorithmic and partly-automated approaches, while other atlases use one of these approaches.[31] We visually inspected for accuracy of parcellation to minimize mislabeling of small ROIs, thus ensuring a high-quality parcellation. Using the HCP-atlas-based ROIs allows for a more granular mapping of gene expression to structurally and functionally connected cortical regions for future investigations. We recently published the results of structural covariance network analysis on the same cohort as a first step.[84] One study using the Desikan–Killiany-Tourville atlas did not find correlation of CT with SZ risk gene expression profiles. Utilizing the HCP atlas, we were able to find correlations between gene expression and alternations in CT. These findings included 10 SZ GWAS genes. Additionally, prior studies examined the association of publicly available gene expression data with morphometry,[24,27] white matter,[23] and functional[42,85] connectivity. Some prior

studies focused on association of cell-type specific genes with CT in adolescents[24] and on SZ risk genes and white matter dysconnectivity in SZ,[23] we examined correlation of expression of all genes agnostic to the association with SZ followed by examining the GWAS significance of the correlated genes. We used a standardized published workflow[32,33] to aid in future replications and reproducibility of the findings. Statistical analyses included appropriate covariates and correction for multiple comparisons minimizing false positive findings.

Limitations of our study include modest sample size and gene expression data from a different cohort than the morphometric measurements making it difficult to directly correlate gene expression with morphometric features. There are known limitations to using microarray data, such as the arrays providing an indirect measure of relative concentration and may capture the expression over a range of concentrations of expression. Microarray data may not reveal all splice variants, and, in the complex human genome, the arrays show the expression of the genes that were known a priori. Recent methods such as RNS-seq may overcome these limitations, but these procedures have their own limitations in terms of cost and the requirement of very stringent quality control. RNA-seq data on the whole-brain is not yet fully available. Notwithstanding these weaknesses, this study highlights expression of different sets of genes and molecular pathways associated with CT in FEAP that can be further investigated for pathophysiology and development of new treatments.

Acknowledgments

We thank the faculty and staff of the Clinical Services Core of the Conte Center for the Neuroscience of Mental Disorders (P50 MH045156, Lewis) for their assistance in diagnostic and psychopathological assessments. *Conflict of Interest*: None of the authors have any conflict of interest relevant to the study and the results in this manuscript.

Funding

This study was supported by the National Institute of Mental Health (NIMH) through R01MH112584 and R01MH115026 (KMP); P50MH045156 (David Lewis), Behavioral Neuroscience and Schizophrenia; and NIH/NCRR/GCRC M01RR00056 (Levine).

References

1. Gottesman II, Shields J. A critical review of recent adoption, twin, and family studies of schizophrenia: behavioral genetics perspectives. *Schizophr Bull.* 1976;2(3):360–401.
2. Sullivan PF, Kendler KS, Neale MC. Schizophrenia as a complex trait: evidence from a meta-analysis of twin studies. *Arch Gen Psychiatry.* 2003;60(12):1187–1192.
3. Wellcome Trust Case Control C. Genome-wide association study of 14,000 cases of seven common diseases and 3,000 shared controls. *Nature.* 2007;447(7145):661–678.
4. Roalf DR, Ruparel K, Verma R, Elliott MA, Gur RE, Gur RC. White matter organization and neurocognitive performance variability in schizophrenia. *Schizophr Res.* 2013;143(1):172–178.
5. Prasad KM, Gertler J, Tollefson S, *et al.* Heritable anisotropy associated with cognitive impairments among patients with schizophrenia and their non-psychotic relatives in multiplex families. *Psychol Med.* 2022;52(5):989–1000.
6. Blokland GA, McMahon KL, Thompson PM, Martin NG, de Zubicaray GI, Wright MJ. Heritability of working memory brain activation. *J. Neurosci.* 2011;31(30):10882–10890.
7. Yokley JL, Prasad KM, Chowdari KV, *et al.* Genetic associations between neuregulin-1 SNPs and neurocognitive function in multigenerational, multiplex schizophrenia families. *Psychiatric Genetics*. 2012;22(2):70–81.
8. Prasad K, Chowdari K, Nimgaonkar V, Talkowski M, Lewis D, Keshavan M. Genetic polymorphisms of the RGS4 and dorsolateral prefrontal cortex morphometry among first episode schizophrenia patients. *Molecular psychiatry*. 2005;10(2):213–219.
9. Goldman AL, Pezawas L, Mattay VS, *et al.* Heritability of brain morphology related to schizophrenia: a large-scale automated magnetic resonance imaging segmentation study. *Biol Psychiatry.* 2008;63(5):475–483.
10. Roalf DR, Vandekar SN, Almasy L, *et al.* Heritability of subcortical and limbic brain volume and shape in multiplex-multigenerational families with schizophrenia. *Biol Psychiatry.* Jan 15 2015;77(2):137–146.
11. Turner JA, Calhoun VD, Michael A, *et al.* Heritability of multivariate gray matter measures in schizophrenia. *Twin Res. Hum. Genet.* 2012;15(3):324–335.
12. Nicodemus KK, Kolachana BS, Vakkalanka R, *et al.* Evidence for statistical epistasis between catechol-O-methyltransferase (COMT) and polymorphisms in RGS4, G72 (DAOA), GRM3, and DISC1: influence on risk of schizophrenia. *Hum Genet.* 2007;120(6):889–906.
13. Cao H, Zhou H, Cannon TD. Functional connectome-wide associations of schizophrenia polygenic risk. *Mol Psychiatry.* 2021;26:2553–2561.
14. Bishop JR, Reilly JL, Harris MS, *et al.* Pharmacogenetic associations of the type-3 metabotropic glutamate receptor (GRM3) gene with working memory and clinical symptom response to antipsychotics in first-episode schizophrenia. *Psychopharmacology (Berl).* 2015;232(1):145–154.
15. Lencer R, Bishop JR, Harris MS, *et al.* Association of variants in DRD2 and GRM3 with motor and cognitive function in first-episode psychosis. *Eur Arch Psychiatry Clin Neurosci.* 2014;264(4):345–355.
16. Stevenson JM, Reilly JL, Harris MS, *et al.* Antipsychotic pharmacogenomics in first episode psychosis: a role for glutamate genes. *Transl Psychiatry.* 2016;6:e739.
17. Wassink TH, Epping EA, Rudd D, *et al.* Influence of ZNF804a on brain structure volumes and symptom severity in individuals with schizophrenia. *Arch Gen Psychiatry.* 2012;69(9):885–892.
18. Wang Z, Chen W, Cao Y, *et al.* An independent, replicable, functional and significant risk variant block at intron 3 of CACNA1C for schizophrenia. *Aust N Z J Psychiatry.* 2021;56(4):385–397.
19. Zheng F, Cui Y, Yan H, Liu B, Jiang T. The effects of a genome-wide supported variant in the CACNA1C gene on

cortical morphology in schizophrenia patients and healthy subjects. *Sci Rep.* 2016;6:34298.

20. Ardesch DJ, Libedinsky I, Scholtens LH, Wei Y, van den Heuvel MP. Convergence of brain transcriptomic and neuroimaging patterns in schizophrenia, bipolar disorder, autism spectrum disorder, and major depressive disorder. *Biol Psychiatry Cogn Neurosci Neuroimaging*. 2023;8(6):630–639.
21. Consortium SWGPG. Biological insights from 108 schizophrenia-associated genetic loci. *Nature.* 2014;511(7510):421–427.
22. Whitaker KJ, Vertes PE, Romero-Garcia R, *et al.*; NSPN Consortium. Adolescence is associated with genomically patterned consolidation of the hubs of the human brain connectome. *Proc Natl Acad Sci USA.* 2016;113(32):9105–9110.
23. Romme IA, de Reus MA, Ophoff RA, Kahn RS, van den Heuvel MP. Connectome disconnectivity and cortical gene expression in patients with schizophrenia. *Biol Psychiatry.* 2017;81(6):495–502.
24. Shin J, French L, Xu T, *et al.* Cell-specific gene-expression profiles and cortical thickness in the human brain. *Cereb Cortex.* 2018;28(9):3267–3277.
25. Autism Spectrum D, Bipolar D, *et al.*; Writing Committee for the Attention-Deficit/Hyperactivity D. Virtual histology of cortical thickness and shared neurobiology in 6 psychiatric disorders. *JAMA Psychiatry.* 2021;78(1):47–63.
26. Di Biase MA, Geaghan MP, Reay WR, *et al.* Cell type-specific manifestations of cortical thickness heterogeneity in schizophrenia. *Mol Psychiatry.* 2022;27(4):2052–2060.
27. Xu X, Li Q, Qian Y, *et al.* Genetic mechanisms underlying gray matter volume changes in patients with drug-naive first-episode schizophrenia. *Cereb Cortex.* 2023;33(5):2328–2341.
28. Chenn A, Walsh CA. Regulation of cerebral cortical size by control of cell cycle exit in neural precursors. *Science.* 2002;297(5580):365–369.
29. Kingsbury MA, Rehen SK, Contos JJ, Higgins CM, Chun J. Non-proliferative effects of lysophosphatidic acid enhance cortical growth and folding. *Nat Neurosci.* 2003;6(12):1292–1299.
30. Prasad KM, Goradia D, Eack S, *et al.* Cortical surface characteristics among offspring of schizophrenia subjects. *Schizophr Res.* 2010;116(2-3):143–151.
31. Glasser MF, Coalson TS, Robinson EC, *et al.* A multi-modal parcellation of human cerebral cortex. *Nature.* 2016;536(7615):171–178.
32. Arnatkeviciute A, Fulcher BD, Fornito A. A practical guide to linking brain-wide gene expression and neuroimaging data. *Neuroimage.* 2019;189:353–367.
33. Markello RD, Arnatkeviciute A, Poline JB, Fulcher BD, Fornito A, Misic B. Standardizing workflows in imaging transcriptomics with the abagen toolbox. *Elife* 2021;10:e72129.
34. Morgan SE, Seidlitz J, Whitaker KJ, *et al.* Cortical patterning of abnormal morphometric similarity in psychosis is associated with brain expression of schizophrenia-related genes. *Proc Natl Acad Sci USA.* 2019;116(19):9604–9609.
35. Bitanihirwe BK, Woo TU. Oxidative stress in schizophrenia: an integrated approach. *Neurosci Biobehav Rev.* 2011;35(3):878–893.
36. Kolar D, Kleteckova L, Brozka H, Vales K.Mini-review: brain energy metabolism and its role in animal models of depression, bipolar disorder, schizophrenia and autism. *Neurosci Lett.* 2021;760:136003.
37. Fornito A, Arnatkeviciute A, Fulcher BD. Bridging the gap between connectome and transcriptome. *Trends Cogn Sci.* 2019;23(1):34–50.
38. Prasad KM, Eack SM, Goradia DD, *et al.* Progressive grey matter loss and changes in cognitive functions associated with exposure to HSV1 in schizophrenia: a longitudinal study. *Am J Psychiatry.* 2011;168(8):822–830.
39. Glasser MF, Smith SM, Marcus DS, *et al.* The Human Connectome Project's neuroimaging approach. *Nat Neurosci.* 2016;19(9):1175–1187.
40. Mills K. *HCP-MMP1.0 projected on fsaverage*; FigShare (dataset). 2016.
41. Bhagwat N, Barry A, Dickie EW, *et al.* Understanding the impact of preprocessing pipelines on neuroimaging cortical surface analyses. *GigaScience.* 2021;10(1):giaa155.
42. Hawrylycz M, Miller JA, Menon V, *et al.* Canonical genetic signatures of the adult human brain. *Nat Neurosci.* 2015;18(12):1832–1844.
43. Fulcher BD, Fornito A. A transcriptional signature of hub connectivity in the mouse connectome. *Proc Natl Acad Sci USA.* 2016;113(5):1435–1440.
44. Benjamini Y, Hochberg Y. Controlling the false discovery rate - a practical and powerful approach to multiple testing. *J R Stat Soc B.* 1995;57(1):289–300.
45. Qiagen. Canonical Pathways for a Dataset. https://qiagen.secure.force.com/KnowledgeBase/articles/Basic_Technical_Q_A/Canonical-Pathways-for-a-Dataset, accessed on December 16, 2021.
46. Trubetskoy V, Pardinas AF, Qi T, *et al.*; Indonesia Schizophrenia Consortium. Mapping genomic loci implicates genes and synaptic biology in schizophrenia. *Nature.* 2022;604(7906):502–508.
47. Panizzon MS, Fennema-Notestine C, Eyler LT, *et al.* Distinct genetic influences on cortical surface area and cortical thickness. *Cereb Cortex.* 2009;19(11):2728–2735.
48. Rakic P. Specification of cerebral cortical areas. *Science.* 1988;241(4862):170–176.
49. Carlo CN, Stevens CF. Structural uniformity of neocortex, revisited. *Proc Natl Acad Sci USA.* 2013;110(4):1488–1493.
50. Ren H, Meng Y, Zhang Y, *et al.* Spatial Expression Pattern of ZNF391 gene in the brains of patients with schizophrenia, bipolar disorders or major depressive disorder identifies new cross-disorder biotypes: a trans-diagnostic, top-down approach. *Schizophr Bull.* 2021;47(5):1351–1363.
51. Del Casale A, Rossi-Espagnet MC, Napolitano A, *et al.* Cerebral cortical thickness and gyrification changes in first-episode psychoses and multi-episode schizophrenia. *Arch Ital Biol.* 2021;159(1):3–20.
52. Goldman AL, Pezawas L, Mattay VS, *et al.* Widespread reductions of cortical thickness in schizophrenia and spectrum disorders and evidence of heritability. *Arch Gen Psychiatry.* 2009;66(5):467–477.
53. Janssen J, Reig S, Aleman Y, *et al.* Gyral and sulcal cortical thinning in adolescents with first episode early-onset psychosis. *Biol Psychiatry.* 2009;66(11):1047–1054.
54. Kuo SS, Roalf DR, Prasad KM, *et al.* Age-dependent effects of schizophrenia genetic risk on cortical thickness and cortical surface area: evaluating evidence for neurodevelopmental and neurodegenerative models of schizophrenia. *J Psychopathol Clin Sci.* 2022;131(6):674–688.
55. Kuo SS, Musket CW, Rupert PE, *et al.* Age-dependent patterns of schizophrenia genetic risk affect cognition. *Schizophr Res.* 2022;246:39–48.

56. Kose M, Pariante CM, Dazzan P, Mondelli V. The role of peripheral inflammation in clinical outcome and brain imaging abnormalities in psychosis: a systematic review. *Front Psychiatry.* 2021;12:612471.
57. Williams JA, Burgess S, Suckling J, *et al.*; PIMS Collaboration. Inflammation and brain structure in schizophrenia and other neuropsychiatric disorders: a mendelian randomization study. *JAMA Psychiatry.* 2022;79(5):498–507.
58. Caspi A, Moffitt TE, Cannon M, *et al.* Moderation of the effect of adolescent-onset cannabis use on adult psychosis by a functional polymorphism in the catechol-O-methyltransferase gene: longitudinal evidence of a gene X environment interaction. *Biol Psychiatry.* 2005;57(10):1117–1127.
59. Prasad KM, Bamne MN, Shirts BH, *et al.* Grey matter changes associated with host genetic variation and exposure to Herpes Simplex Virus 1 (HSV1) in first episode schizophrenia. *Schizophr Res.* 2010;118(1–3):232–239.
60. Lener MS, Goodnow SJ, Wood JA, *et al.* RGS4 and COMT risk variants are associated with brain structural alterations. *Schizophr Res.* 2013;150(1):321–322.
61. Song X, Chen X, Yuksel C, *et al.* Bioenergetics and abnormal functional connectivity in psychotic disorders. *Mol Psychiatry.* 2021;26(6):2483–2492.
62. Duarte JMN, Xin L. Magnetic resonance spectroscopy in schizophrenia: evidence for glutamatergic dysfunction and impaired energy metabolism. *Neurochemical Res*. 2019;44(1):102–116.
63. Mazgaj R, Tal A, Goetz R, *et al.* Hypo-metabolism of the rostral anterior cingulate cortex associated with working memory impairment in 18 cases of schizophrenia. *Brain Imaging Behav.* 2016;10(1):115–123.
64. Nenadic I, Dietzek M, Langbein K, *et al.* Superior temporal metabolic changes related to auditory hallucinations: a (31) P-MR spectroscopy study in antipsychotic-free schizophrenia patients. *Brain Structure Function.* 2014;219(5):1869–1872.
65. Calabrese G, Deicken RF, Fein G, Merrin EL, Schoenfeld F, Weiner MW. 31Phosphorus magnetic resonance spectroscopy of the temporal lobes in schizophrenia. *Biol Psychiatry.* 1992;32(1):26–32.
66. Deicken RF, Calabrese G, Merrin EL, Vinogradov S, Fein G, Weiner MW. Asymmetry of temporal lobe phosphorous metabolism in schizophrenia: a 31phosphorous magnetic resonance spectroscopic imaging study. *Biol Psychiatry.* 1995;38(5):279–286.
67. Karry R, Klein E, Ben Shachar D. Mitochondrial complex I subunits expression is altered in schizophrenia: a postmortem study. *Biol Psychiatry.* 2004;55(7):676–684.
68. Maurer I, Zierz S, Moller H. Evidence for a mitochondrial oxidative phosphorylation defect in brains from patients with schizophrenia. *Schizophr Res.* 2001;48(1):125–136.
69. Schmitt A, Malchow B, Hasan A, Falkai P. The impact of environmental factors in severe psychiatric disorders. *Front Neurosci* . 2014;8:19.
70. Smrt RD, Zhao X. Epigenetic regulation of neuronal dendrite and dendritic spine development. *Frontiers Biol.* 2010;5(4):304–323.
71. Boni C, Laudanna C, Sorio C. A Comprehensive Review of Receptor-Type Tyrosine-Protein Phosphatase Gamma (PTPRG) role in health and non-neoplastic disease. *Biomolecules.* 2022;12(1):84.
72. Carli M, Kolachalam S, Longoni B, *et al.* Atypical antipsychotics and metabolic syndrome: from molecular mechanisms to clinical differences. *Pharmaceuticals (Basel).* 2021;14(3):238.
73. Kim P, Scott MR, Meador-Woodruff JH. Abnormal ER quality control of neural GPI-anchored proteins via dysfunction in ER export processing in the frontal cortex of elderly subjects with schizophrenia. *Transl Psychiatry.* 2019;9(1):6.
74. Kunii Y, Matsumoto J, Izumi R, *et al.* Evidence for altered phosphoinositide signaling-associated molecules in the postmortem prefrontal cortex of patients with schizophrenia. *Int J Mol Sci* . 2021;22(15):8280.
75. Mitsunaga C, Mikami T, Mizumoto S, Fukuda J, Sugahara K. Chondroitin sulfate/dermatan sulfate hybrid chains in the development of cerebellum. Spatiotemporal regulation of the expression of critical disulfated disaccharides by specific sulfotransferases. *J Biol Chem.* 2006;281(28):18942–18952.
76. Ceccom J, Loukh N, Lauwers-Cances V, *et al.* Reduced sphingosine kinase-1 and enhanced sphingosine 1-phosphate lyase expression demonstrate deregulated sphingosine 1-phosphate signaling in Alzheimer's disease. *Acta Neuropathol Commun*. 2014;2:12.
77. Martin KW, Weaver N, Alhasan K, *et al.* MRI spectrum of brain involvement in sphingosine-1-phosphate lyase insufficiency syndrome. *AJNR Am J Neuroradiol.* 2020;41(10):1943–1948.
78. Alvarez SE, Milstien S, Spiegel S. Autocrine and paracrine roles of sphingosine-1-phosphate. *Trends Endocrinol Metab.* 2007;18(8):300–307.
79. Olsen ASB, Faergeman NJ. Sphingolipids: membrane microdomains in brain development, function and neurological diseases. *Open Biol.* 2017;7(5):1–17.
80. Haszto CS, Stanley JA, Iyengar S, Prasad KM. Regionally distinct alterations in membrane phospholipid metabolism in schizophrenia: a meta-analysis of phosphorus magnetic resonance spectroscopy studies. *Biol Psychiatry Cogn Neurosci Neuroimaging.* 2020;5(3):264–280.
81. Prasad KM, Burgess A, Nimgaonkar VL, Keshavan MS, Stanley JA. Neuropil pruning in early-course schizophrenia: immunological, clinical and neurocognitive correlates. *BP:CNNI*. 2016;1(6):528–538.
82. Prasad KM, Chowdari KV, D'Aiuto LA, Iyengar S, Stanley JA, Nimgaonkar VL. Neuropil contraction in relation to Complement C4 gene copy numbers in independent cohorts of adolescent-onset and young adult-onset schizophrenia patients-a pilot study. *Transl Psychiatry.* 2018;8(1):134.
83. Desikan RS, Segonne F, Fischl B, *et al.* An automated labeling system for subdividing the human cerebral cortex on MRI scans into gyral based regions of interest. *Neuroimage.* 2006;31(3):968–980.
84. Lewis M, Santini T, Theis N, *et al.* Modular architecture and resilience of structural covariance networks in first-episode antipsychotic-naive psychoses. *Sci Rep.* 2023;13(1):7751.
85. Anderson KM, Krienen FM, Choi EY, Reinen JM, Yeo BTT, Holmes AJ. Gene expression links functional networks across cortex and striatum. *Nat Commun.* 2018;9(1):1428.